Human serum triggers antibiotic tolerance in *Staphylococcus aureus*

Elizabeth V. K. Ledger[1], Stéphane Mesnage[2] and Andrew M. Edwards[1#]

[1] MRC Centre for Molecular Bacteriology and Infection, Imperial College London, Armstrong Rd, London, SW7 2AZ, UK.

[2] School of Biosciences, University of Sheffield, Sheffield, S10 2TN, UK.

[#] For correspondence:
a.edwards@imperial.ac.uk

Keywords: *Staphylococcus aureus* / daptomycin / antibiotic tolerance / peptidoglycan / cardiolipin / serum / AMP

Running title: Serum triggers antibiotic tolerance

Abstract

Staphylococcus aureus is a frequent cause of bloodstream infections. Treatment can be challenging, even when isolates appear to be drug susceptible, with high rates of persistent and relapsing infection. This is particularly the case with infections caused by methicillin resistant *S. aureus* (MRSA) strains, which are resistant to frontline antibiotics. To understand how the host environment influences treatment outcomes in MRSA infections, we studied the impact of human serum on staphylococcal susceptibility to daptomycin, an antibiotic of last resort. This revealed that serum triggered a very high degree of tolerance to daptomycin, as well as several other classes of antibiotics and antimicrobial peptides, including gentamicin, nitrofurantoin, vancomycin, nisin and gramicidin. Serum-induced daptomycin tolerance was due to two independent mechanisms. Firstly, the host defence peptide LL-37 present in serum induced tolerance by triggering the staphylococcal GraRS two component system. This led to increased cell wall accumulation that reduced access of daptomycin to its membrane target. Secondly, GraRS-independent changes to the membrane resulted in increased cardiolipin abundance that also contributed to daptomycin tolerance. When both mechanisms were blocked, serum exposed *S. aureus* cells were as susceptible to daptomycin as bacteria growing in laboratory media. These data demonstrate that host factors can significantly modulate antibiotic susceptibility via diverse mechanisms, which may in turn contribute to treatment failure. The inhibition of serum-induced cell wall accumulation by fosfomycin reduced tolerance, suggesting that this antibiotic may form a useful combination therapy with daptomycin.

Introduction

S. aureus is a leading cause of invasive infections, resulting in over 12,000 cases of bacteraemia each year in the UK[1]. The choice of treatment depends on the antibiotic susceptibility of the pathogen, with infections caused by methicillin sensitive *S. aureus* (MSSA) usually treated with front-line β-lactams such as oxacillin. However, there are few effective therapeutic options for invasive infections caused by methicillin resistant *S. aureus* (MRSA) strains, with the recommended treatments including vancomycin and daptomycin[2].

Daptomycin, a cyclic lipopeptide antibiotic approved to treat MRSA bacteraemia in 2003, targets membrane phosphatidylglycerol (PG) and permeabilises bacterial membranes[3]. This leads to a loss of intracellular ions and ATP, as well as disruption to the cell wall biosynthetic and division machinery[3]. *In vitro*, daptomycin is highly potent and rapidly bactericidal but this potency is not observed *in vivo*, where despite giving high doses intravenously, it can take several days to sterilise the bloodstream[4,5]. This slow rate of clearance allows *S. aureus* to disseminate around the body, leading to the development of secondary infections[6], such as infective endocarditis, osteomyelitis, septic arthritis, meningitis and tissue abscesses[7]. As a result, patients require long hospital stays, leading to high treatment costs, and suffer from high mortality rates[8,9]. Specifically, daptomycin fails to cure 20 – 30 % cases of MRSA bacteraemia and is associated with a 10 – 20 % mortality rate[4,5,10,11]. Therefore, it is important to understand why treatment failure occurs so that new approaches can be developed to improve patient survival rates.

Although daptomycin resistance (typically referred to as non-susceptibility) can occur during therapy, it is not the only explanation for treatment failure and in many patients failure occurs despite the infecting strain being classed as susceptible by antimicrobial susceptibility testing[12,13]. In these cases, a possible explanation for treatment failure is antibiotic tolerance, where a bacterial population survives exposure to a normally lethal concentration of an antibiotic without an increase in minimum inhibitory concentration (MIC)[14]. This tolerance can be due to mutations[15–17] or phenotypic adaptation, a transient phenotype which is thought to be induced by the environment conditions, especially those found in the host[12,13] As the population returns to a susceptible state when it is removed from the host environment, this tolerance is difficult to detect *in vitro* but may play an important role clinically[18]. Furthermore, there is growing evidence that tolerance is a precursor to the acquisition of antibiotic resistance[19].

The mechanisms responsible for antibiotic tolerance are poorly understood although it is frequently ascribed to slow rates of bacterial growth and/or low metabolic activity[12,20]. These are thought to compromise the activity of antibiotics that require bacterial division for full activity such as β-lactams

and quinolones. However, as daptomycin is effective against non-growing bacteria[21], this is unlikely to be the basis of the reduced efficacy of daptomycin *in vivo* and the mechanisms of tolerance towards daptomycin remain unknown.

Although the causes of antibiotic tolerance are not fully understood, there is growing evidence that it can be transiently induced by the host environment during infection. For example, the numerous stresses found in the host, such as nutrient limitation, low pH, pyrexia, oxidative and/or nitrosative stress, antimicrobial peptides and proteases, mean that bacteria are rarely in a rapidly replicating state[12,22,23]. These stresses may restrict bacterial growth directly, for example hypoxia leading to a switch to anaerobic metabolism, which produces less energy than the TCA cycle, or indirectly, for example nutrient limitation activating the stringent response[24–26]. This response results in downregulation of expression of genes required for growth, leading to a reduction in protein synthesis and a slower bacterial growth rate[24]. This has been linked to the development of tolerance towards a range of antimicrobials including penicillin, vancomycin and ciprofloxacin[27].

In addition to restricted bacterial growth rates due to hostile conditions, activation of other bacterial stress responses by host factors has also been implicated in antibiotic tolerance[28,29] and the formation of multidrug tolerant states, including persister cells and SCVs[30–32]. However, it is not clear whether the mechanisms by which induction of stress responses lead to drug tolerant states is simply due to a reduction in growth or metabolic activity or whether there are other mechanisms involved.

Unfortunately, many of these host-associated stresses are typically not replicated in laboratory culture media, meaning that antibiotic tolerance is difficult to detect and is often missed. Laboratory media lack host-derived nutrients and macromolecules, resulting in significant differences between the metabolism and physiology of *S. aureus in vitro* and *in vivo*. Additionally, phenotypic studies have identified that growth in model host environments affects properties of the staphylococcal cell envelope, including affecting the structure of the cell wall and the composition and properties of the cell membrane[33–35]. For example, incorporation of serum unsaturated fatty acids affected membrane fluidity, a factor known to influence the susceptibility of *S. aureus* to membrane-targeting antimicrobials[34,36]. However, the impact of such changes on antibiotic susceptibility have not been tested.

Therefore, although there is an increasing awareness that the host environment affects many aspects of *S. aureus* physiology and metabolism, the impact this has on antibiotic susceptibility and the mechanisms involved is poorly understood. Using human serum as a model host environment of

bacteraemia, we discovered two novel mechanisms by which host defences induce daptomycin tolerance and identified a possible combination therapeutic approach to enhance antibiotic efficacy.

Results

Incubation of *S. aureus* in serum results in daptomycin tolerance

Since daptomycin is frequently used to treat *S. aureus* bloodstream infections,[1,37] we used normal human serum as an *ex vivo* model to examine how the host environment affected daptomycin susceptibility. In this model, we performed antibiotic bactericidal activity assays on *S. aureus* in two states: i) grown to mid-exponential phase in tryptic soy broth (TSB) to represent *in vitro* conditions ("TSB-grown") and ii) incubated for 16 h in human serum to mimic host conditions ("serum-adapted"; Fig. 1A). In agreement with previous reports[38], colony forming unit (CFU) counts of *S. aureus* did not change during the 16 h incubation in serum (Fig. S1). Therefore, equal numbers of *S. aureus* CFU from TSB-grown and serum-adapted cultures were exposed to daptomycin. To control for any effects that serum had directly on the antibiotic, for example via protein binding, bacterial survival assays of both TSB-grown and serum-adapted cultures were performed in serum (Fig. 1A).

When TSB-grown *S. aureus* were challenged with a range of clinically achievable concentrations of daptomycin (up to 80 μg ml^{-1}; equivalent to peak serum concentrations observed in patients[39]), dose and time-dependent killing over 6 h was observed (Fig. 1B). There were lower levels of bacterial survival at higher daptomycin concentrations and later time points, confirming that TSB-grown *S. aureus* was susceptible to daptomycin and that despite serum protein binding, high levels of killing were achieved in serum (Fig. 1B).

By contrast, when serum-adapted *S. aureus* were exposed to daptomycin, killing was completely abolished at both 20 and 40 μg ml^{-1} daptomycin, while 17 % of the initial inoculum survived exposure to 80 μg ml^{-1} daptomycin (Fig. 1B). Therefore, at 80 μg ml^{-1} daptomycin, serum adaptation led to a > 200,000-fold increase in bacterial survival compared to TSB-grown *S. aureus*.

Next, we tested whether this serum-induced tolerance was unique to daptomycin or whether it also occurred with other classes of antimicrobial. Serum adaptation conferred tolerance towards two representative antimicrobial peptides (AMPs), nisin and gramicidin, demonstrating that serum adaptation was able to protect *S. aureus* not only from daptomycin but also other membrane-targeting antimicrobials (Fig. S2A – B). Moreover, serum adaptation resulted in high levels of tolerance towards three additional bactericidal antibiotics with diverse mechanisms of action, vancomycin (cell wall synthesis inhibition), nitrofurantoin (DNA damage) and gentamicin (protein synthesis inhibition) (Fig. S2C – E).

166 Taken together, adaptation to the host environment conferred high levels of tolerance towards the
167 last-resort antibiotic daptomycin. Serum also induced tolerance towards other membrane-targeting
168 antimicrobials with a similar mechanism of action to daptomycin and also towards more diverse
169 antibiotics with various modes of killing.

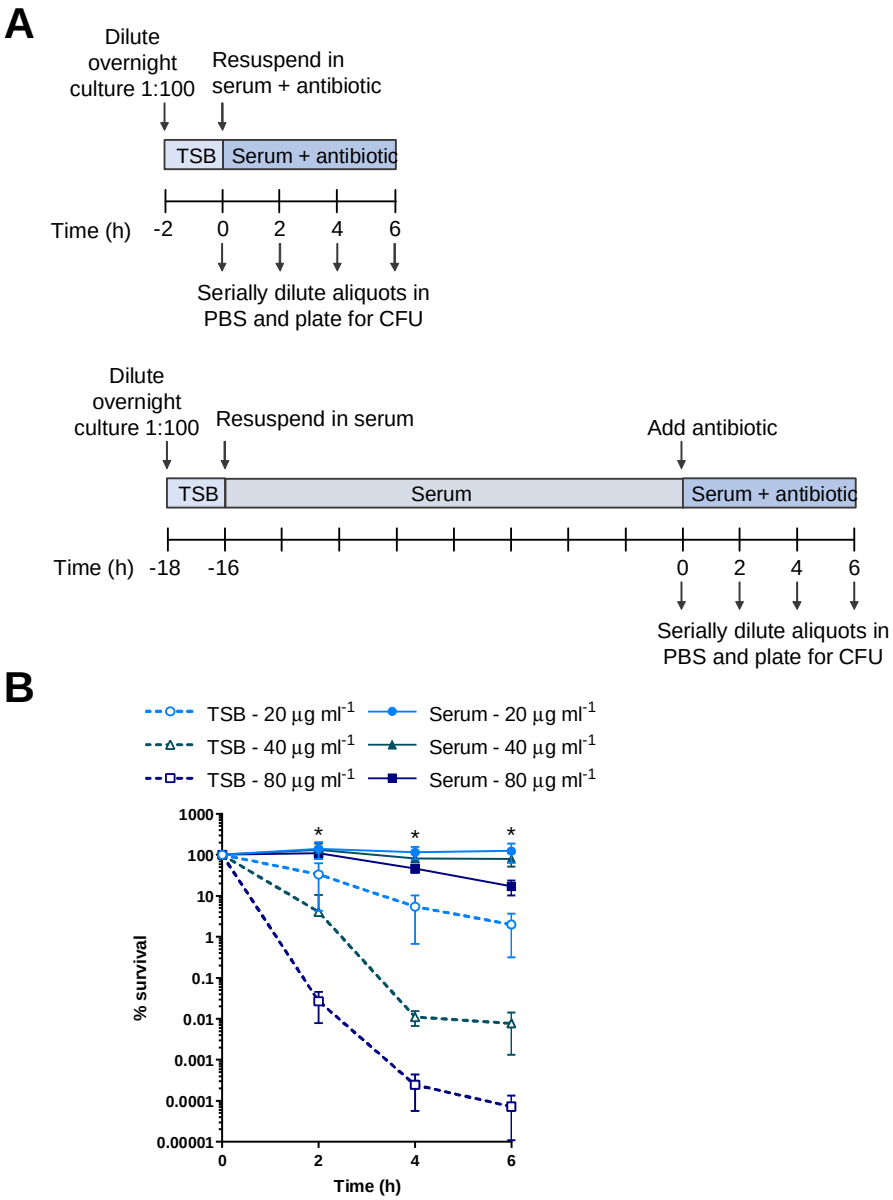

170

171 **Figure 1. Incubation of *S. aureus* in serum results in tolerance towards daptomycin.** Schematic
172 outlining the protocol used to investigate the susceptibility of TSB-grown and serum-adapted
173 cultures of *S. aureus* to daptomycin (**A**). Percentage survival of TSB-grown and serum-adapted
174 cultures of *S. aureus* USA300 WT over 6 h incubation in serum with 20 – 80 µg ml^{-1} daptomycin (**B**).
175 Graph represents the mean ± standard deviation of three independent experiments. (*, $P < 0.05$

two-way ANOVA with Tukey's *post-hoc* test, TSB-grown compared to serum-adapted at each time-point).

Daptomycin does not bind to or disrupt the membranes of *S. aureus* incubated in serum

Despite potent activity *in vitro*, daptomycin is associated with high rates of relapse and mortality, possibly due to the tolerance phenotype described above[4,5,10,11]. We therefore decided to determine the mechanism by which adaptation to serum conferred daptomycin tolerance and thereby identify opportunities to enhance treatment efficacy.

Following calcium-dependent binding of daptomycin to PG, daptomycin oligomers form in the membrane, leading to membrane disruption, loss of intracellular ions and ATP and cell death[3]. Therefore, we first determined whether incubation in serum prevented daptomycin from interacting with its bacterial membrane target. To do this, TSB-grown and serum-adapted cells were exposed to the fluorescent BoDipy-labelled daptomycin in serum, and aliquots taken at each time point to measure the levels of cell-associated antibiotic. A large increase in the fluorescence of TSB-grown cultures was observed during the first 2 h, followed by a gradual increase over the following 4 h (Fig. 2A). By contrast, a smaller increase in fluorescence during the first 2 h was observed with serum-adapted *S. aureus*, with no further increase after this time point, indicating reduced binding of daptomycin to serum-adapted bacteria compared to TSB-grown cells (Fig. 2A). Aliquots taken at the 2 h time point were fixed, co-stained with the lipophilic dye Nile Red to visualise cell membranes and analysed by fluorescence microscopy. In agreement with Fig. 2A, this demonstrated that *S. aureus* were bound by higher levels of BoDipy-daptomycin when in a TSB-grown state than in a serum-adapted state (Fig. 2B).

Next, we determined whether serum adaptation protected *S. aureus* from daptomycin-induced membrane disruption. To do this, we measured membrane potential using the voltage-sensitive fluorescent dye $DiSC_3(5)$[40] and the ability of *S. aureus* to exclude propidium iodide (PI) as an indication of membrane permeability. TSB-grown and serum-adapted cultures of *S. aureus* were exposed, or not, to 80 μg ml^{-1} daptomycin for 6 h in human serum and then $DiSC_3(5)$ or PI was added and the fluorescence measured. In each case, exposure of TSB-grown cells to daptomycin led to a significant increase in fluorescence compared to untreated cells, demonstrating that daptomycin resulted in membrane depolarisation and permeabilisation (Fig. 2C – D). By contrast, there was no significant increase in the fluorescence of serum-adapted bacteria after exposure to daptomycin, showing that serum adaptation prevented daptomycin-induced membrane damage (Fig. 2C – D).

Taken together, these results indicated that high levels of daptomycin bound to TSB-grown *S. aureus,* resulting in membrane permeabilisation, depolarisation and rapid cell death. By contrast, incubation of *S. aureus* in serum resulted in daptomycin tolerance by significantly reducing the

amount of daptomycin that bound to the membrane and thereby greatly reducing the associated membrane damage and cell death.

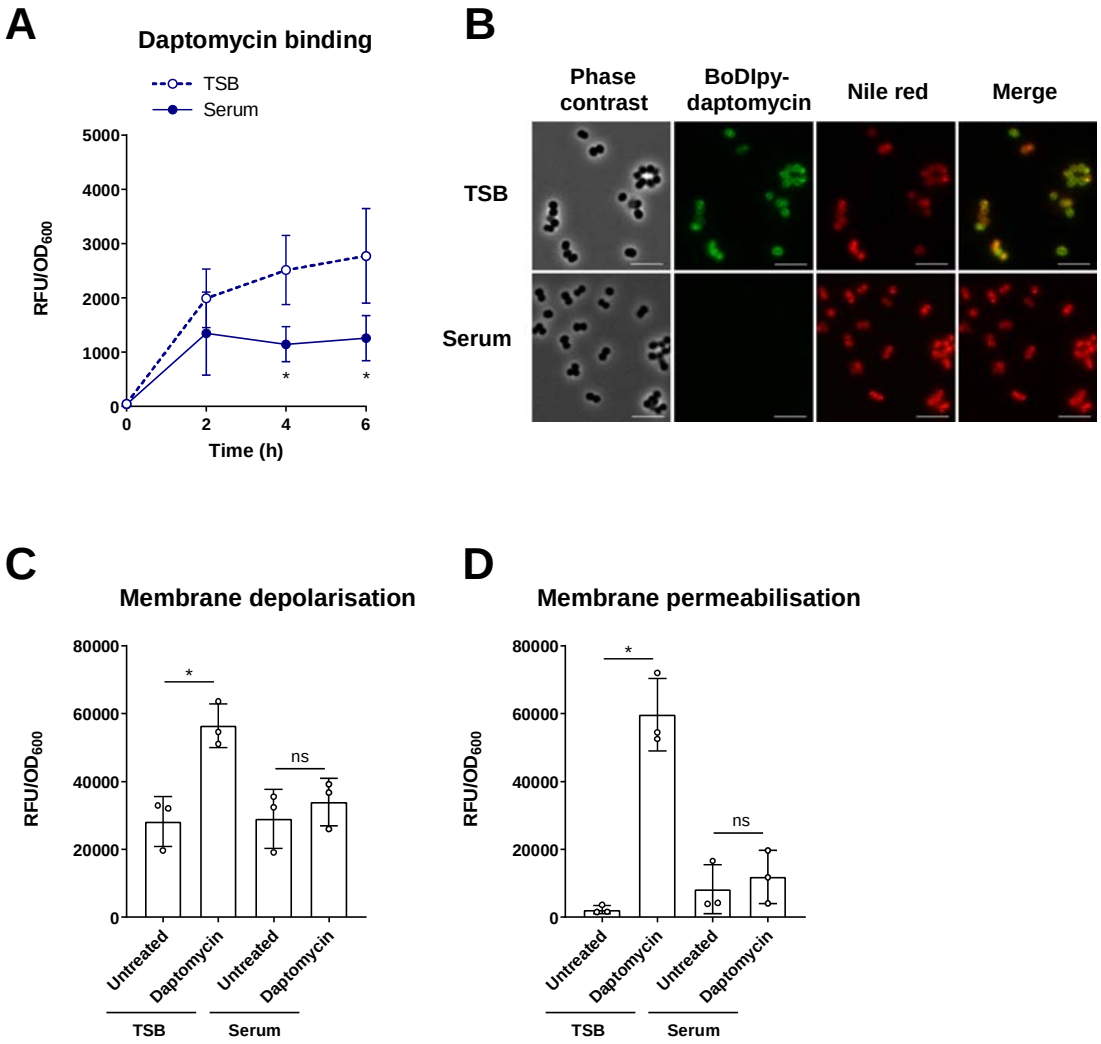

Figure 2. Daptomycin does not bind to or disrupt the membranes of *S. aureus* incubated in serum. Cell-associated fluorescence of TSB-grown and serum-adapted cultures of *S. aureus* USA300 WT over a 6 h incubation with 320 µg ml^{-1} BoDipy-daptomycin (**A**). Cells after 2 h daptomycin exposure from panel **A** were fixed and analysed by phase contrast and fluorescence microscopy (**B**). Cells were co-stained with 10 µg ml^{-1} nile red to visualise cell membranes. Scale bars, 5 µm. $DiSC_3(5)$ (**C**) and propidium iodide (**D**) fluorescence of TSB-grown and serum-adapted cultures. Fluorescence values were divided by OD_{600} measurements to normalise for changes in cell density which occurred throughout the assays. Graphs represent the mean ± standard deviation of three independent experiments. *, $P < 0.05$. Data in **A** were analysed by two-way ANOVA with Sidak's *post-hoc* test

(TSB-grown vs serum-adapted at each time-point. Data in **C** and **D** were analysed by two-way ANOVA with Tukey's *post-hoc* test (untreated vs daptomycin-exposed).

LL-37 in serum triggers daptomycin tolerance through activation of the GraRS two-component system

The next aim was to identify the specific factor(s) in serum responsible for triggering daptomycin tolerance and the staphylococcal system(s) activated. Since two-component systems (TCS) are a key mechanism for sensing many environmental signals, we carried out a screen of mutants in each non-essential TCS in the *S. aureus* USA300 genome to determine whether any were required for serum-induced tolerance[41]. To do this, serum-adapted cultures of *S. aureus* JE2 WT and transposon mutants defective for each sensor kinase were exposed to 80 μg ml^{-1} daptomycin for 6 h and survival measured by CFU counts. As expected, serum adaptation conferred daptomycin tolerance on the WT strain (Fig. 3A). By contrast, mutants defective for VraS or GraS showed ~100-fold lower levels of survival compared to WT (Fig. 3A). Complementation of the *graS*::Tn and *vraS*::Tn mutant strains with *graXRS* or *vraUTSR* respectively expressed from their native promoters on a low copy number plasmid completely restored daptomycin tolerance to WT levels (Fig. S3A – B).

Next, we determined whether either of the VraSR or GraRS signalling systems were activated by serum. To do this, fluorescent reporters were constructed, where the expression of *gfp* was placed under the control of a promoter of a gene regulated by either TCS. To measure induction of VraSR and GraRS signalling, the *vraX* and *dltA* promoters were used as these are known to be regulated by VraSR and GraRS respectively[42–44]. Strains containing these reporter constructs were exposed to human serum and fluorescence measured over time. An increase in *vraX* expression was not detected on exposure to serum in either the WT or *vraS*::Tn mutant background, providing no evidence that serum induced signalling of this system (Fig. 3B). By contrast, when the WT strain containing the GraRS reporter was exposed to serum there was a rapid increase in GFP fluorescence over the first 3 h, but no change in the fluorescence of the *graS*::Tn mutant reporter strain (Fig. 3C), indicating that serum triggered GraRS signalling in *S. aureus*.

To investigate whether activation of GraRS was capable of inducing daptomycin tolerance, we induced signalling by incubation of *S. aureus* in RPMI 1640 supplemented with sub-inhibitory concentrations of colistin, a known trigger of GraRS[44] (Fig. S4A). RPMI 1640 was chosen as it is a host-mimicking cell culture medium that lacks the factor present in serum that activates GraRS. Exposure of the P*dltA-gfp* reporter strains to colistin led to dose-dependent production of GFP in the WT strain but not in the *graS*::Tn mutant (Fig. S4A), confirming that colistin was triggering GraRS. Next, *S. aureus* was incubated for 16 h in RPMI 1640 supplemented, or not, with colistin and then exposed to daptomycin. Incubation in media alone did not confer daptomycin tolerance, with just

0.1 % of the initial inoculum surviving exposure to the antibiotic (Fig. S4B). Supplementation of RPMI 1640 with colistin led to dose dependent increases in bacterial survival in the WT strain, with the highest concentration of colistin triggering a 70-fold increase in survival of the inoculum, relative to bacteria not exposed to colistin (Fig. S4B). By contrast, no significant increase in survival was seen in the *graS*::Tn mutant when incubated in RPMI 1640 containing colistin, compared to media alone (Fig. S4B).

Next, we investigated whether GraRS signalling could be inhibited pharmacologically to block the development of daptomycin tolerance. Verteporfin is a licenced photosensitising drug used to treat macular degeneration which has been reported to also inhibit GraS[45]. Bacterial adaptation was carried out in serum, or serum supplemented with sub-lethal concentrations of verteporfin, before cultures were exposed to daptomycin. Consistent with a role for GraRS in daptomycin tolerance, incubation of *S. aureus* in serum in the presence of verteporfin led to a dose-dependent decrease in tolerance, which resulted in 100-fold increase in bacterial killing when 80 µg ml^{-1} verteporfin was used (Fig. 3D). By contrast, supplementation of serum with verteporfin had no significant effect on the tolerance of the *graS*::Tn mutant to daptomycin (Fig. 3D).

Next, we aimed to identify the signal in serum responsible for activating GraRS signalling and thereby daptomycin tolerance. As GraRS is activated by certain AMPs[46], we tested a range of peptides present in serum to identify the trigger of tolerance. To do this, the P*dltA-gfp* reporter strains were exposed to sub-inhibitory concentrations of AMPs and the ability of each AMP to trigger GraRS activation was determined. LL-37 led to dose-dependent induction of GraRS in the WT background (Fig. 3E). For example, at 8 h, 20, 40 and 80 µg ml^{-1} LL-37 led to 1.6-, 2.7- and 3.6-fold increases in *dltA* expression respectively compared to samples not exposed to LL-37 (Fig. 3E). By contrast, no induction was observed in the *graS*::Tn mutant (Fig. 3E). Human neutrophil peptide-1 (hNP-1) and platelet AMPs did not induce GraRS signalling, while dermcidin only induced signalling very weakly (Fig. S5A – C).

To determine whether LL-37 induced daptomycin tolerance, JE2 WT and *graS*::Tn strains were incubated for 16 h in RPMI 1640 alone, or supplemented with various sub-inhibitory concentrations of LL-37, before addition of daptomycin. Incubation in media alone did not confer daptomycin tolerance, but as the concentration of LL-37 increased, the daptomycin tolerance of the WT strain also increased, with up to 200-fold increased survival of bacteria incubated with the highest LL-37 concentration compared with medium without peptide (Fig. 3F). By contrast, no increase in survival of the *graS*::Tn mutant was observed on addition of LL-37 (Fig. 3F). In agreement with the reporter data, neither hNP-1, dermcidin nor platelet AMPs triggered daptomycin tolerance (Fig. S5D – F).

Finally, to confirm that serum LL-37 was responsible for triggering tolerance in serum, a sheep polyclonal anti-LL-37 IgG antibody was assessed for its ability to prevent the induction of daptomycin tolerance in *S. aureus.* As a negative control, serum was pre-incubated with a sheep IgG targeting hNP-1, a peptide which did not activate GraRS signalling or trigger daptomycin tolerance (Fig. S5A, D). In the absence of antibody pre-incubation, high levels of daptomycin tolerance were observed, however, as the concentration of anti-LL-37 antibody increased, the ability of the serum to induce daptomycin tolerance decreased in a dose-dependent manner (Fig. 3G). By contrast, pre-incubation with the anti-hNP-1 antibody had no effect on daptomycin tolerance at any of the concentrations used (Fig. 3G).

Taken together, these data demonstrate that serum triggered daptomycin tolerance via LL-37 mediated activation of GraRS signalling.

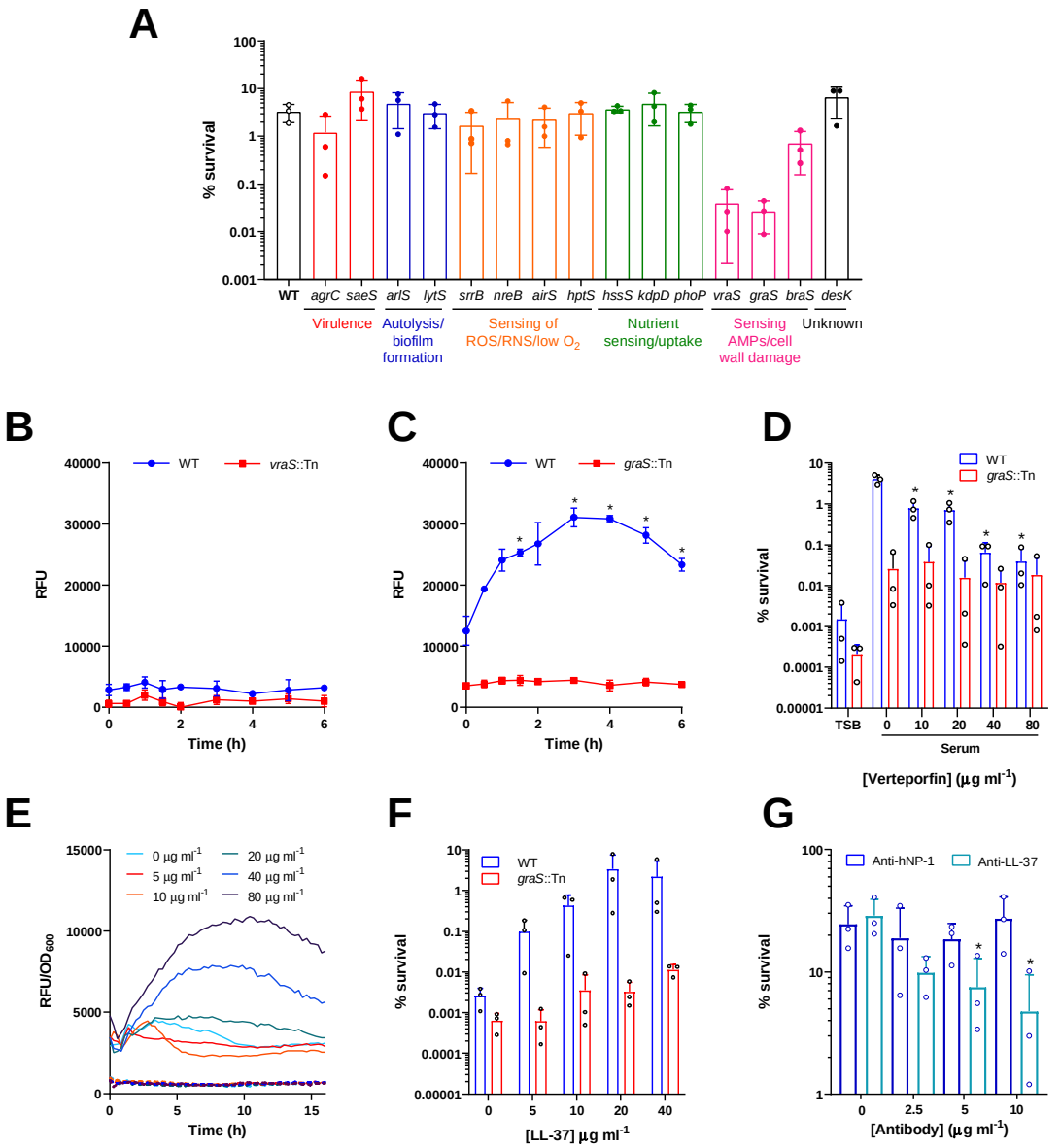

Figure 3. LL-37 in serum triggers daptomycin tolerance through activation of the GraRS two-component system. Percentage survival of serum-adapted cultures of *S. aureus* JE2 WT and transposon mutants defective for the sensor components of various TCS after 6 h incubation with 80 µg ml^{-1} daptomycin (**A**). GFP fluorescence over a 6 h exposure of TSB-grown cultures of *S. aureus* JE2 WT and the *vraS*::Tn mutant containing P*vraX-gfp* (**B**) or JE2 WT and the *graS*::Tn mutant containing *PdltA-gfp* (**C**) to human serum. Percentage survival after 6 h exposure to 80 µg ml^{-1} daptomycin of *S. aureus* JE2 WT and the *graS*::Tn mutant which had been TSB-grown or pre-incubated for 16 h in serum supplemented with indicated concentrations of verteporfin (**D**). TSB-grown cultures of *S. aureus* JE2 WT (solid lines) and the *graS*::Tn mutant (dashed lines) containing P*dltA-gfp* were

exposed to various concentrations of LL-37 (5 – 80 μg ml^{-1}) in RPMI 1640 and GFP fluorescence (RFU) and OD_{600} were measured every 15 min for 16 h (**E**). Fluorescence values were divided by OD_{600} measurements to normalise for changes in cell density. Percentage survival of WT and *graS*::Tn mutant strains which had been incubated for 16 h in RPMI 1640 supplemented with indicated concentrations of LL-37 and then exposed to 80 μg ml^{-1} daptomycin for 6 h (**F**). Percentage survival of *S. aureus* JE2 WT incubated for 16 h in serum supplemented with indicated concentrations of antibody targeting hNP-1 or LL-37 and then exposed to 80 μg ml^{-1} daptomycin for 6 h. All graphs represent the mean ± standard deviation of three independent experiments except panel **E** where error bars have been omitted for clarity. Data in **A** were analysed by one-way ANOVA (WT vs mutants). Data in **B** and **C** were analysed by two-way ANOVA with Dunnett's *post-hoc* test (*, $P < 0.05$, RFU at each time-point compared to 0 h). Data in **D**, **F** and **G** were analysed by two-way ANOVA with Dunnett's *post-hoc* test (*, $P < 0.05$, serum + verteporfin/LL-37/antibody compared to serum alone). RFU, relative fluorescence units; hNP-1, human neutrophil peptide 1.

GraRS-mediated changes in surface charge do not explain serum-induced tolerance

The next aim was to determine how activation of GraRS by serum conferred daptomycin tolerance. GraRS regulates many genes, including those encoding the lysyl-phosphatidylglycerol (LPG) synthase and flippase, MprF, and the DltABCD system, which modifies teichoic acids with D-alanine[46–48]. Upregulation of these genes results in an increase in positive surface charge, which has been proposed to reduce daptomycin susceptibility through charge-mediated repulsion[49].

Therefore, we measured the surface charge of TSB-grown and serum-adapted cultures of *S. aureus* using a fluorescently labelled cationic molecule, fluorescein isothiocyanate-poly-L-lysine (FITC-PLL). TSB-grown and serum-adapted cultures were incubated with FITC-PLL, washed to remove unbound dye and fixed. Analysis of the fluorescence of the surface of individual cells demonstrated that serum-adapted bacteria bound significantly less FITC-PLL, and so were more positively charged, than TSB-grown cells (Fig. 4A).

Next, we aimed to determine whether either of the main systems involved in modulating surface charge in *S. aureus,* MprF or DltABCD, were required for tolerance. To do this, TSB-grown and serum-adapted cultures of mutants in each system (*mprF*::Tn and *ΔdltD*, respectively) were exposed to 80 μg ml^{-1} daptomycin and survival compared to WT strains. Neither mutant was more susceptible to daptomycin than WT when in a TSB-grown state (Fig. 4B – C). Serum adaptation conferred daptomycin tolerance on the *mprF*::Tn mutant, with survival of 100 % of the mutant population

344 observed at 6 h (Fig. 4B). By contrast, serum adaptation did not protect the *ΔdltD* mutant from
345 daptomycin, with a 1000-fold reduction in CFU counts after 6 h exposure to the antibiotic (Fig. 4C).
346 This defect in daptomycin tolerance was fully complemented by the expression of *dltD* on a plasmid
347 from its native promoter (Fig. S6). Therefore, teichoic acid D-alanylation, but not LPG synthesis, was
348 required for daptomycin tolerance in serum.

349 To explore the requirement for teichoic acid D-alanylation for tolerance further, we next determined
350 whether incubation in serum affected the amount of wall teichoic acid (WTA) present or the degree
351 to which it was modified. To do this, WTA was extracted from TSB-grown and serum-adapted
352 cultures of *S. aureus,* analysed by native polyacrylamide gel electrophoresis (PAGE), visualised by
353 alcian blue staining and quantified. This demonstrated two-fold higher levels of WTA in serum-
354 adapted than TSB-grown bacteria (Fig. 4D). The levels of D-alanine present in WTA extracts were
355 quantified using an enzyme-based spectrophotometric assay, demonstrating a three-fold increase in
356 the D-alanine content of serum-adapted cells compared to TSB-grown (Fig. 4E). Finally, to investigate
357 whether this increase in D-alanylated WTA was mediating tolerance, TSB-grown cultures were
358 incubated for 16 h in serum supplemented, or not, with one of three WTA synthesis inhibitors,
359 before addition of daptomycin and measurement of survival. Supplementation of serum with either
360 tarocin A1 or tunicamycin completely prevented the increase in D-alanylated WTA which occurred
361 during serum adaptation (Fig. 4D – E). However, this inhibition did not affect serum-mediated
362 daptomycin tolerance (Fig. 4F), demonstrating that despite D-alanylated WTA being required for
363 tolerance, the increase in this modified polymer observed in serum was not responsible for
364 tolerance.

365

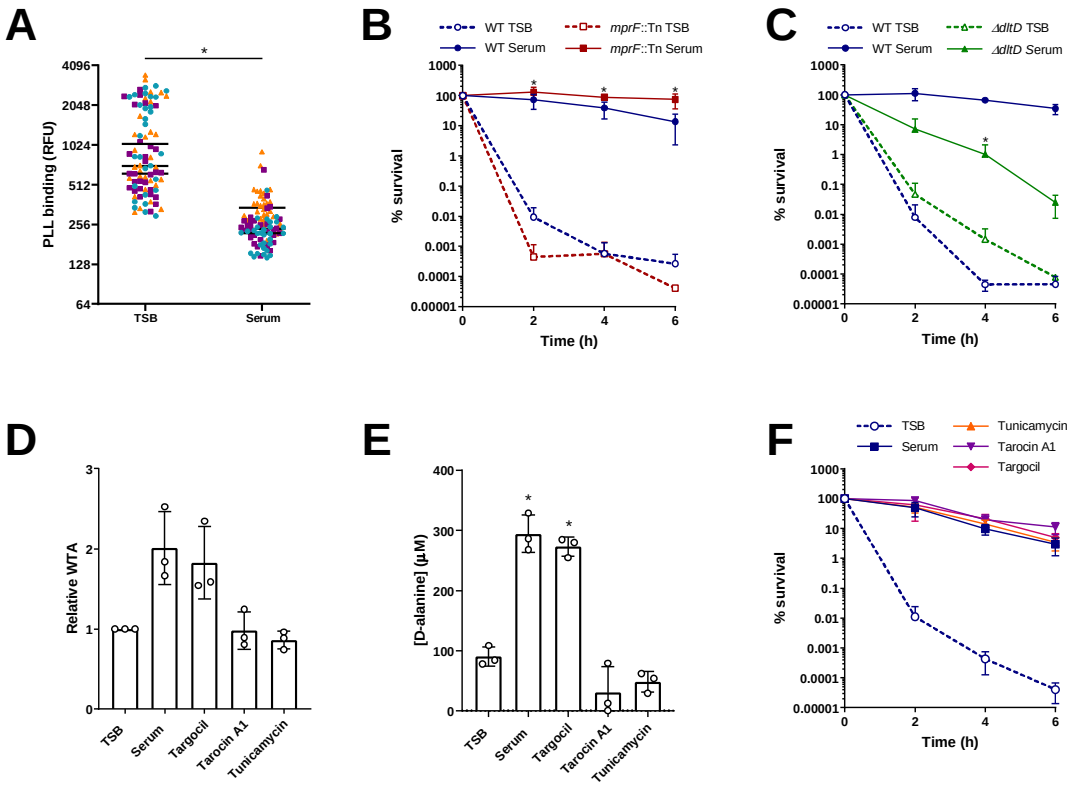

Figure 4. GraRS-mediated changes in surface charge do not explain serum-induced tolerance. FITC-PLL binding to TSB-grown and serum-adapted cultures *S. aureus* JE2 WT. Cultures were incubated with 80 μg ml^{-1} FITC-PLL, washed, fixed and analysed by fluorescence microscopy (**A**). The fluorescence of 30 cells per biological replicate (90 cells total per condition) was measured and the mean of each replicate is indicated. Colours represent different biological replicates. Percentage survival of TSB-grown and serum-adapted cultures of *S. aureus* JE2 WT and the *mprF*::Tn mutant (**B**) and the *ΔdltD* mutant (**C**) during a 6 h exposure to 80 μg ml^{-1} daptomycin in serum (**B**). WTA extracts from TSB-grown bacteria and cultures incubated in serum supplemented, or not, with 128 μg ml^{-1} targocil, 64 μg ml^{-1}, tarocin A1 or 128 μg ml^{-1} tunicamycin for 16 h were analysed by native PAGE with alcian blue staining and quantified using ImageJ (**D**). Concentrations of D-alanine in WTA extracts from panel **D** were determined spectrophotometrically using an enzyme-based assay and by interpolating values from a standard curve generated from known D-alanine concentrations (**E**). Percentage survival over 6 h exposure to 80 μg ml^{-1} daptomycin of TSB-grown *S. aureus* or cultures which had been incubated in serum supplemented, or not, with 128 μg ml^{-1} targocil, 64 μg ml^{-1} tarocin A1 or 128 μg ml^{-1} tunicamycin for 16 h (**F**). Data in **A** were analysed by a Mann-Whitney test (*, $P < 0.05$). Data in **B** and **C** were analysed by two-way ANOVA with Tukey's *post-hoc* test (*, $P < 0.05$, serum-adapted WT vs serum-adapted mutant at each time-point). Data in **D** and **E** were analysed by one-way ANOVA with Dunnett's *post-hoc* test (*, $P < 0.05$, TSB-grown vs serum-

385 adapted). Data in **F** were analysed by two-way ANOVA (serum + WTA synthesis inhibitor vs serum
386 alone; no statistically significant differences were observed). FITC-PLL, fluorescein isothiocyanate-
387 poly-L-lysine.

388 **GraRS-mediated changes to the cell wall partially explain serum-induced tolerance**

389 Having ruled out the MprF-mediated synthesis of LPG and the DltABCD-mediated increase in D-
390 alanylated WTA as direct causes of serum-induced daptomycin tolerance, we next investigated
391 whether other GraRS-regulated genes mediated tolerance. As many genes involved in cell wall
392 metabolism, including several peptidoglycan hydrolytic enzymes[47,50], are regulated by GraRS we
393 tested whether there were differences in the peptidoglycan layer between TSB-grown and serum-
394 adapted *S. aureus*.

395 Cell walls were extracted from TSB-grown and serum-adapted bacteria, the WTA removed by acid
396 hydrolysis and the resulting peptidoglycan freeze-dried and its mass determined. This demonstrated
397 that serum-adapted *S. aureus* contained approximately 5-fold more peptidoglycan than TSB-grown
398 cells (Fig. 5A). This accumulation of peptidoglycan during incubation in serum was partially
399 dependent on GraRS as serum-adaptation led to a smaller increase in the peptidoglycan content of
400 the *graS*::Tn mutant strain (~2-fold) (Fig. 5A). To corroborate these findings, a fluorescent approach
401 was developed to evaluate the peptidoglycan content by measuring the incorporation of a
402 fluorescent D-amino acid analogue, HADA[51]. This analogue is incorporated into the pentapeptide
403 stem of peptidoglycan by *S. aureus* in the place of D-alanine[51] and so provides a measure of the
404 amount of peptidoglycan synthesised during the incubation with HADA. TSB-grown and serum-
405 adapted *S. aureus* were generated in the presence of HADA, fixed, analysed by fluorescence
406 microscopy and quantified (Fig. 5B). In agreement with the data in Fig. 5A, this revealed that serum-
407 adapted WT *S. aureus* showed > 5-fold higher levels of fluorescence than TSB-grown bacteria and
408 this increase in HADA fluorescence was reduced in the absence of *graS* (Fig. 5B). Furthermore,
409 similar results were seen with the Δ*dltD* mutant, which had significantly lower levels of
410 peptidoglycan compared WT cells after incubation in serum, explaining why D-alanylation of WTA
411 was needed for serum-induced daptomycin tolerance (Fig. S6, S7).

412 We next investigated whether incubation in serum resulted in peptidoglycan modifications mediated
413 by the GraRS TCS. Peptidoglycan was purified from WT and *graS*::Tn cells grown in TSB or following
414 serum adaptation and the corresponding muropeptide profiles were analysed by rp-HPLC (Fig. 5C).
415 When grown in TSB, no differences were detected between the WT and the *graS*::Tn mutant (Fig.
416 5C). As expected, incubation in serum resulted in additional peaks, likely resulting from the activity
417 of human-derived peptidoglycan hydrolases present in serum[52]. However, these additional peaks

418 were present in both the WT and *graS*::Tn mutant samples (Fig. 5C). Collectively, these data suggest
419 that incubation in serum does not result in GraRS-mediated peptidoglycan modifications.

420 Finally, we investigated whether the increased peptidoglycan of serum-adapted cells contributed to
421 daptomycin tolerance. To do this, *S. aureus* were incubated in serum supplemented with a sub-lethal
422 concentration of fosfomycin, a peptidoglycan synthesis inhibitor (Fig. S8). As expected, this
423 prevented the increase in HADA fluorescence triggered by serum (Fig. 5D). In line with earlier results,
424 serum-adaptation resulted in daptomycin tolerance in untreated bacteria (Fig. 5E). By contrast,
425 supplementation of serum with fosfomycin reduced tolerance, with ~200-fold fewer CFU surviving 6
426 h daptomycin exposure (Fig. 5E).

427 Taken together, these findings demonstrated that serum-adaptation conferred tolerance via a
428 GraRS-dependent increase in peptidoglycan content.

429

430

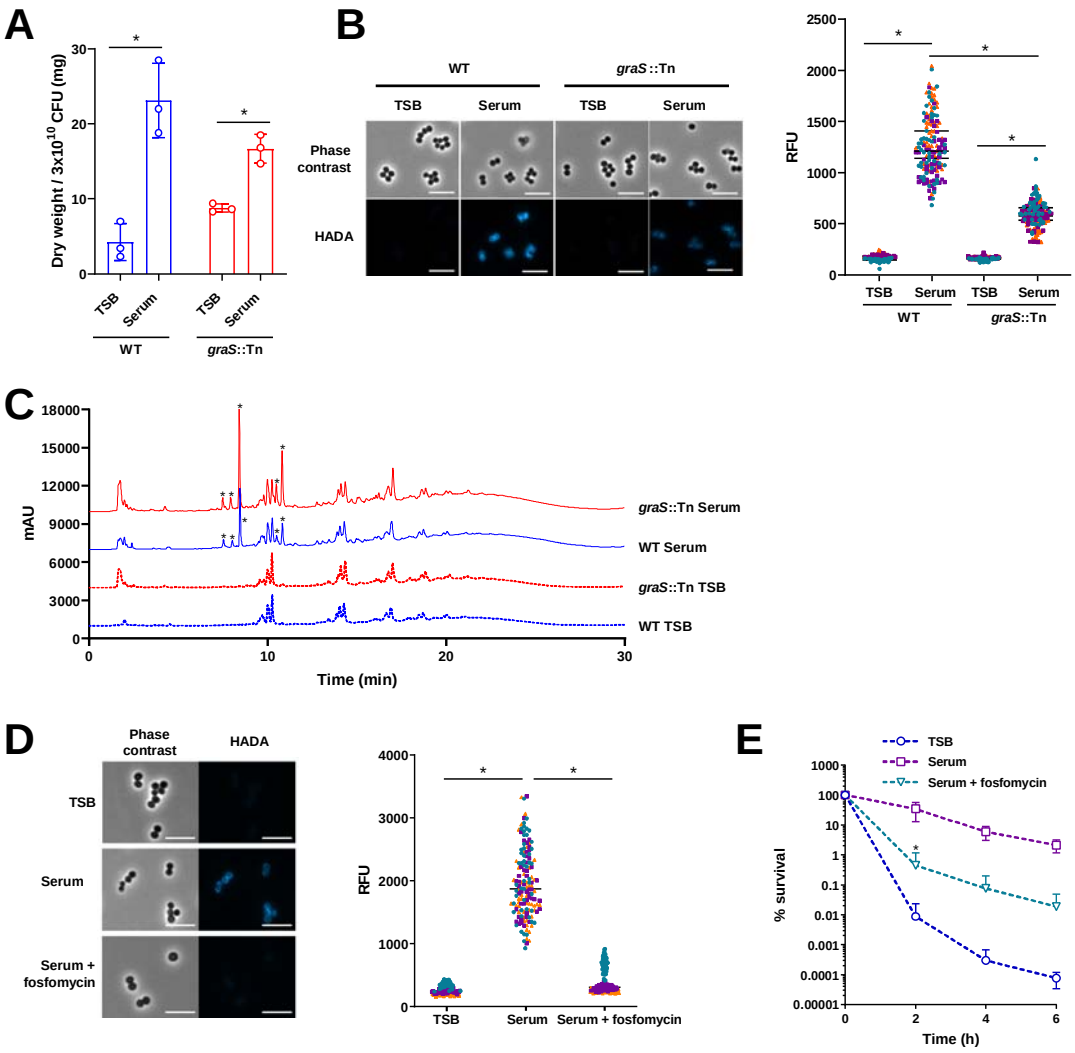

Figure 5. GraRS-mediated increase in peptidoglycan partially explains serum-induced tolerance. Dry weight of peptidoglycan extracted from 300 ml cultures of TSB-grown or serum-adapted *S. aureus* JE2 WT or the *graS*::Tn mutant strain (**A**). Phase contrast and fluorescence microscopy of TSB-grown and serum-adapted cultures of *S. aureus* WT and the *graS*::Tn mutant strain (**B**). Scale bars, 5 µm. The fluorescence of individual cells was quantified. Graph represents the fluorescence of 50 cells per biological replicate (150 cells in total) with the mean of each replicate indicated. Each biological replicate is depicted in a different colour. Peptidoglycan from panel **A** was analysed by rp-HPLC (**C**). Asterisks denote peaks present in serum-adapted but not TSB-grown samples. Phase contrast and fluorescence microscopy of TSB-grown, serum-adapted or serum + 64 µg ml^{-1} fosfomycin-adapted cultures of *S. aureus* JE2 WT (**D**). Scale bars, 5 µm. The fluorescence of individual cells was quantified and different colours represent different biological replicates. Percentage survival of bacteria depicted in panel **D** during a 6 h exposure to 80 µg ml^{-1} daptomycin in serum (**E**). Graphs in **A** and **E** represent the mean ± standard deviation of three independent experiments. Data

445 in **A** were analysed by two-way ANOVA with Sidak's *post-hoc* test. Data in **B** and **D** were analysed by
446 Kruskal-Wallis with Dunn's *post hoc* test. Data in **E** were analysed by two-way ANOVA with Dunnett's
447 *post-hoc* test (*, $P < 0.05$; serum-adapted vs serum/fosfomycin-adapted at each time-point).

448

449 **Accumulation of peptidoglycan is associated with a GraRS-dependent reduction in**
450 **hydrolytic activity**

451 The total amount of peptidoglycan depends on the balance between cell wall synthesis and
452 degradation. As GraRS regulates several peptidoglycan hydrolases[47,50], we hypothesised that
453 incubation in serum led to cell wall accumulation in part via a reduction in the rate of cell wall
454 degradation. To test this, we measured rates of Triton-X-mediated autolysis. This showed that TSB-
455 grown *S. aureus* lysed rapidly on exposure to Triton X-100, resulting in 37 % of the initial optical
456 density remaining after 6 h (Fig. 6A). By contrast, serum-adapted bacteria underwent significantly
457 less lysis, with 93 % of the initial optical density remaining after 6 h (Fig. 6A). Next, we carried out
458 zymography to determine the abundance and activity of the hydrolytic enzymes present in the cell
459 wall. Several bands corresponding to enzymes with hydrolytic activity were visible in the TSB-grown
460 sample, whereas there were fewer and weaker bands in cell walls isolated from serum-adapted
461 samples (Fig. 6B). This reduced hydrolytic activity was dependent on GraRS as serum-adapted
462 cultures of the *graS*::Tn mutant underwent significantly more Triton-X-triggered lysis than the WT
463 strain (Fig. 6C). This difference in lysis was complemented by the presence of the P*graXRS* plasmid
464 but not by empty pCN34 (Fig. 6C). Additionally, zymography demonstrated that there were more
465 hydrolases present in the sample from serum-adapted cultures of the *graS*::Tn mutant than the WT
466 (Fig. 6D). These bands were also present in the wall extracts of the mutant strain complemented
467 with empty pCN34 but were not observed when the mutant was complemented with P*graXRS* (Fig.
468 6D).

469 Taken together, serum-adapted *S. aureus* showed a GraRS-dependent decrease in hydrolytic activity
470 compared to TSB-grown cultures, suggesting that the serum-induced accumulation of peptidoglycan
471 was partly due to a reduction in the rate at which the cell wall was being degraded.

472

473

474

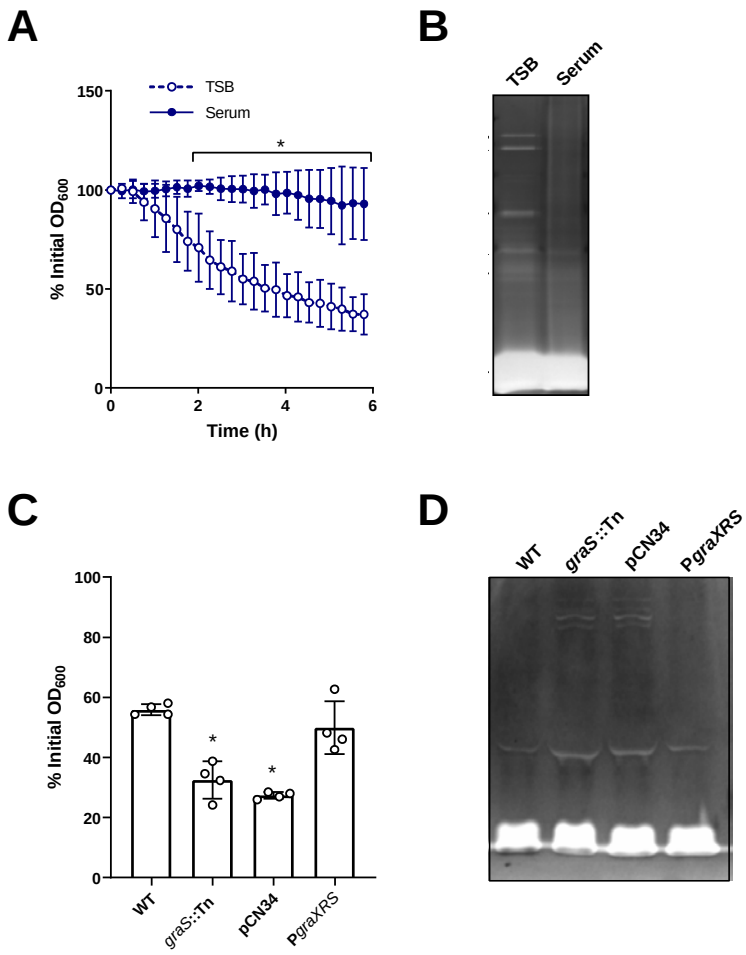

Figure 6. Accumulation of peptidoglycan is associated with a GraRS-dependent reduction in autolysis. Triton X-100-triggered lysis of TSB-grown and serum-adapted cultures of *S. aureus* as measured by following OD_{600} values during a 6 h exposure to 0.05 % Triton X-100 (**A**). Cell wall extracts of TSB-grown and serum-adapted *S. aureus* were separated by SDS-PAGE using gels containing heat-killed *S. aureus* cells. Hydrolases were allowed to refold and zones of peptidoglycan degradation were visualised using methylene blue (**B**). Triton X-100-triggered lysis of serum-adapted cultures of *S. aureus* WT, the *graS*::Tn mutant and the *graS*::Tn mutant complemented with empty pCN34 or P*graXRS* as measured by OD_{600} values after a 6 h exposure to 0.05 % Triton X-100 (**C**). Cell wall extracts of serum-adapted cultures of *S. aureus* WT, the *graS*::Tn mutant and the *graS*::Tn mutant complemented with empty pCN34 or P*graXRS* were analysed by zymography (**D**). Graphs in **A** and **C** represent the mean ± standard deviation of three or four independent experiments respectively. Three independent replicates of zymography were carried out and one representative image is shown. Data in **A** were analysed by two-way ANOVA with Sidak's *post-hoc* test; *, $P < 0.05$. Data in **C** were analysed by one-way ANOVA with Dunnett's *post-hoc* test; WT vs mutants.

Full daptomycin tolerance requires GraRS-independent changes to the staphylococcal membrane

While GraRS-dependent changes to peptidoglycan contributed to serum-induced daptomycin tolerance, they did not fully explain it. As the cell membrane is an important determinant of daptomycin susceptibility, we examined whether tolerance was also due to changes in membrane phospholipid composition. Phospholipids were extracted from TSB-grown and serum-adapted cultures using a method based on that of Bligh and Dyer[53]. However, as it has been shown that incubation in serum leads to host phospholipids associating with the staphylococcal membrane[33], cells were washed with Triton X-100 before extraction to remove these non-covalently bound lipids. After phospholipid extraction, thin layer chromatography (TLC) was used to separate phospholipids, which were then visualised with phosphoric acid and copper sulphate[54]. As expected, this analysis showed the three main phospholipid species present in the staphylococcal membrane, cardiolipin (CL), PG and LPG[55]. Quantification showed that serum-adapted *S. aureus* contained significantly more CL (10.3 % total phospholipids vs 7.8 % in TSB-grown cells) and less PG (80 % in TSB vs 75 % in serum) than TSB-grown bacteria (Fig. 7A). Similar changes in phospholipid composition were observed on incubation of the *graS*::Tn mutant in serum, indicating that these changes were not GraRS-dependent (Fig. 7B).

To investigate whether this increase in CL was required for daptomycin tolerance TSB-grown and serum-adapted cultures of JE2 WT and mutants in the two CL synthases present in *S. aureus* (*cls1*::Tn and *cls2*::Tn) were exposed to daptomycin and survival measured. There were no significant differences between the killing kinetics of the strains when TSB-grown, demonstrating that the susceptibilities of the strains to daptomycin were similar (Fig. 7C). As expected, serum adaptation conferred a high level of tolerance on the WT strain, with 58 % of the population surviving 6 h daptomycin exposure (Fig. 7C). Similarly, the *cls1*::Tn mutant also showed high levels of tolerance (Fig. 7C). By contrast, serum adaptation did not protect the *cls2*::Tn mutant from daptomycin, with only 0.4 % of the inoculum surviving after 6 h (Fig. 7C). This defect in daptomycin tolerance was fully complemented by the expression of *cls2* on a plasmid from its native promoter (Fig. S9). As with the WT strain, incubation in serum led to a significant increase in the CL content of the *cls1*::Tn strain and a decrease in PG (Fig. 7D). By contrast, incubation in serum did not significantly affect the membrane composition of the *cls2*::Tn mutant strain, with no differences observed in the content of CL, PG or LPG between TSB-grown and serum-adapted cultures (Fig. 7E). Therefore, in agreement with its requirement for tolerance, Cls2, but not Cls1, was required for the accumulation of CL that occurred during serum adaptation.

While the *cls2*::Tn mutant strain showed significantly reduced tolerance compared to WT, tolerance was not completely abolished in this strain (Fig. 7C). Therefore, the final objective was to determine whether the increase in peptidoglycan and CL together fully explained daptomycin tolerance. To do this, peptidoglycan synthesis was inhibited in the WT strain with fosfomycin, CL accumulation was prevented by using the *cls2*::Tn mutant or synthesis of both molecules was inhibited together by incubating the *cls2*::Tn mutant in serum supplemented with a sub-lethal concentration of fosfomycin. Cultures were then exposed to daptomycin for 6 h and survival measured. Inhibition of either cell wall synthesis or CL accumulation led to small reductions in tolerance (Fig. 7F). Inhibition of both peptidoglycan and CL accumulation together completely abolished daptomycin tolerance, with daptomycin killing these bacteria as efficiently as TSB-grown cultures (Fig. 7F).

Taken together, incubation in serum led to an increase in both peptidoglycan and CL, and inhibition of the synthesis of both these molecules completely prevented daptomycin tolerance.

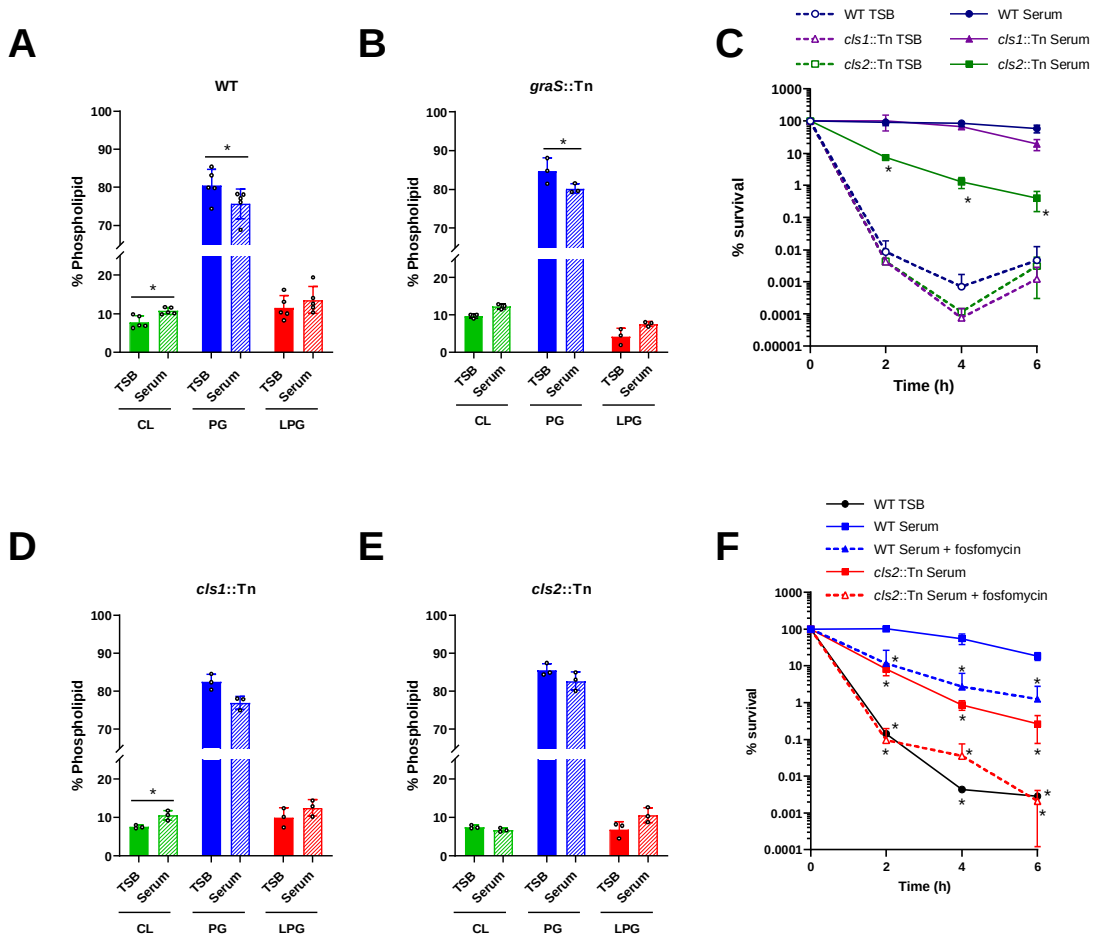

Figure 7. GraRS-independent changes to the staphylococcal membrane also contribute to tolerance. Phospholipids were extracted from TSB-grown and serum-adapted cultures of *S. aureus* JE2 WT (**A**), the *graS*::Tn mutant (**B**), the *cls1*::Tn mutant (**D**) and the *cls2*::Tn mutant (**E**) before being analysed by thin layer chromatography and visualised with copper sulphate and phosphoric acid. The relative phospholipid compositions were determined by quantifying spot intensities using ImageJ. Percentage survival of TSB-grown and serum-adapted cultures of *S. aureus* JE2 WT and the *cls1*::Tn and *cls2*::Tn mutant strains during a 6 h exposure to 80 µg ml^{-1} daptomycin in serum (**C**). Percentage survival of TSB-grown and serum-adapted cultures of *S. aureus* JE2 WT and the *cls2*::Tn mutant strains during a 6 h exposure to 80 µg ml^{-1} daptomycin in serum (**F**). Where appropriate, adaptation was carried out with sub-lethal concentrations of fosfomycin (dashed lines). Graphs represent the mean ± standard deviation of at least three independent experiments. Data in **A**, **B**, **D** and **E** were analysed by paired t-tests (*, $P < 0.05$; TSB-grown vs serum-adapted for each phospholipid). CL, cardiolipin; PG, phosphatidylglycerol; LPG, lysyl-phosphatidylglycerol. Data in **C** and **F** were analysed

by two-way ANOVA with Tukey's *post-hoc* test (*, $P < 0.05$; serum-adapted WT vs serum-adapted mutant/fosfomycin-adapted at each time-point).

Discussion

Treatment of invasive MRSA infections is challenging due to limited effective treatment options. This means that infections are associated with high rates of treatment failure even when they are caused by drug-susceptible strains[12]. Understanding the reasons behind this failure is crucial to improving the efficacy of antibiotic therapy. There is evidence that in some cases, treatment failure may be due to antibiotic tolerance being induced by the host environment, but unfortunately, this tolerance is not observed in standard laboratory media[12]. Using human serum to model bloodstream infections, we demonstrated that adaptation to the host environment induced high levels of tolerance to several bactericidal antibiotics with different mechanisms of action, including vancomycin, gentamicin, nitrofurantoin and the last-resort antibiotic daptomycin.

Serum-triggered daptomycin tolerance was due in part to activation of GraRS by host LL-37, a finding that adds to our growing understanding that triggering of stress responses by the host can enable bacteria to survive antibiotic exposure[12]. LL-37 has previously been identified to promote transient tolerance of *S. aureus* towards vancomycin, contributing to treatment failure in a *Galleria* infection model[29]. Furthermore, colistin exposure has been shown to enable *S. aureus* to grow in the presence of otherwise inhibitory concentrations of vancomycin[23]. Whilst it was not established if vancomycin tolerance was due to activation of GraRS by LL-37 or colistin, there were phenotypic similarities to what we observed, including increased cell wall thickness[23,29].

Serum-induced daptomycin tolerance was due to changes in both the cell wall and the cell membrane, which together prevented daptomycin from binding to its target and causing membrane damage. The serum-induced increase in peptidoglycan was dependent on GraRS, partly due to a decrease in cell wall degradation as incubation in serum led to a GraRS-dependent decrease in the abundance and activity of peptidoglycan hydrolases. Importantly, this increase in peptidoglycan is in line with the results of other studies that have investigated the differences between *S. aureus* grown in culture medium and in model host environments. For example, Hines *et al*. demonstrated that the cell walls of *S. aureus* grown in 20 % human serum were twice as thick as those grown in TSB[33], while Sutton *et al*. observed that the cell walls of *S. aureus* isolated from an experimental murine kidney abscess model were significantly thicker than those of cells grown *in vitro*[35]. Therefore, we are confident that the results from our *ex vivo* model system are applicable to the host environment during infection.

As LL-37 is produced by both macrophages and neutrophils it is likely to be present at many sites of bacterial infection and may therefore contribute to antibiotic tolerance at diverse anatomical sites as well as the bloodstream[56]. Sensing of LL-37 by *S. aureus* is important because this AMP has anti-staphylococcal activity and mutants lacking GraRS are more susceptible to LL-37 and have decreased survival in a murine infection model[57]. Therefore, we hypothesise that GraRS mediated sensing of LL-37 and the resulting cell wall thickening constitutes a defence against LL-37 and other AMPs. In support of this, we found that serum triggered tolerance of the AMPs nisin and gramicidin, as well as daptomycin.

The importance of the peptidoglycan layer in influencing daptomycin susceptibility fits with observations that the thickened cell walls of VISA strains frequently confer reduced susceptibility to daptomycin[58,59]. Additionally, studies of daptomycin non-susceptible (DNS) isolates revealed thicker cell walls in many cases and metabolic studies of DNS isolates demonstrated a shift from glycolysis towards the pentose phosphate pathway which is used to generate precursors for peptidoglycan synthesis[60]. Furthermore, Bertsche *et al.* observed that DNS strains contained higher levels of both WTA and peptidoglycan than susceptible isolates, however, they did not determine which polymer was responsible for the resistance[61,62]. Therefore, our discovery that it is the peptidoglycan rather than the WTA component of the wall which mediates tolerance may inform about the mechanisms used by *S. aureus* to survive daptomycin exposure more broadly.

In addition to changes to the cell wall, serum also induced daptomycin tolerance through alterations in phospholipid composition, specifically, a Cls2-dependent increase in CL and decrease in PG content. Both decreased PG and increased CL have previously been associated with the DNS phenotype[63]. As PG is the target of daptomycin, it is clear why a reduction in this phospholipid may mediate tolerance whereas the mechanism by which increased CL reduces susceptibility is less clear. Increased CL has been reported to reduce the ability of daptomycin and other AMPs to permeabilise model membranes[64,65], while an increased CL content in some DNS isolates has been observed to increase membrane rigidity and thickness, impairing daptomycin penetration and membrane disruption[63].

Accumulation of CL by *S. aureus* in serum was due to Cls2 rather than Cls1. Previous work has shown that Cls2 is the 'housekeeping' CL synthase and responsible for CL accumulation in stationary phase[66]. As such, it is possible that the bacteriostasis conferred upon *S. aureus* by serum mimics stationary phase, leading to Cls2-mediated CL accumulation. Cls2, together with Cls1, is also required for CL accumulation in response to phagocytosis by neutrophils, although it is not known whether LL-37 produced by phagocytic cells triggers this phenomenon[66].

The large differences in TSB-grown and serum-adapted cell envelopes indicate that tolerant cells are in a very different state from drug susceptible bacteria, suggesting that they have undergone significant changes in transcription and metabolism. These findings are in line with those of Peyrusson *et al.*, who studied the transcriptional responses of *S. aureus* persisters inside infected host cells[25]. They found that persisters were metabolically active and showed altered transcription characteristic of the activation of several stress responses, including the stringent response, cell wall stress response and SOS response[25]. Therefore, as is the case when exposed to serum, *S. aureus* can be in a non-replicative state but maintain metabolic and transcriptional activity, highlighting the difference between a lack of growth and a lack of metabolism and demonstrating that metabolic inactivity is not required for daptomycin tolerance.

Understanding the mechanisms behind daptomycin tolerance is important for developing a combination therapeutic approach using readily available drugs as a simple and effective way to improve treatment outcomes. Serum-induced tolerance occurred via two mechanisms: a GraRS-dependent accumulation of peptidoglycan and a GraRS-independent increase in CL. Inhibition of either of these processes significantly reduced the extent of daptomycin tolerance *in vitro*, indicating that targeting these processes may be a viable strategy to reduce tolerance. Unfortunately, although we demonstrated that inhibition of GraRS using verteporfin reduced daptomycin tolerance in serum, this drug is unsuitable for use systemically due to toxicity, and a second GraRS inhibitor, MAC-545496 cannot be used due to poor aqueous solubility[45,67]. Therefore, although inhibition of GraRS may reduce daptomycin tolerance, a lack of suitable inhibitors currently precludes their testing in *in vivo* invasive disease models. Inhibition of CL accumulation is also not currently a viable approach as, to the best of our knowledge, no inhibitors of *S. aureus* Cls2 have been described. By contrast, the finding that peptidoglycan synthesis was essential for host-mediated daptomycin tolerance raises the possibility that combined use of daptomycin with a cell wall synthesis inhibitor may prevent tolerance. In support of this, supplementation of serum with fosfomycin prevented cell wall accumulation and significantly reduced the number of bacteria which survived subsequent daptomycin exposure. As well as preventing tolerance, a combination approach may also have other benefits as fosfomycin has been shown to synergise with daptomycin in *in vitro* and *in vivo* studies and to slow the development of daptomycin resistance[68–72]. The basis of this synergy is thought to be an increase in daptomycin binding, providing additional evidence that the wall acts as a significant barrier for daptomycin and that by reducing cell wall thickness daptomycin can reach its membrane target more easily[73]. Moreover, a randomised trial of patients with MRSA bacteraemia found that the combination of daptomycin and fosfomycin was associated with 12 % higher rate of treatment success than daptomycin monotherapy[4].

In summary, we have described a novel mechanism by which human serum triggers antibiotic tolerance in *S. aureus,* including towards the last resort antibiotic daptomycin. This provides a potential explanation for the relatively low efficacy of daptomycin when used in patients, which contrasts with its potent bactericidal activity *in vitro*. Daptomycin tolerance occurred via two distinct mechanisms: a GraRS-dependent increase in peptidoglycan and an increase in the CL content of the membrane. Inhibition of either of these processes reduced the development of tolerance, providing a rationale for a combination therapeutic approach to prevent daptomycin tolerance and enable the lipopeptide antibiotic to kill *S. aureus* effectively.

Materials and methods

Bacterial strains and growth conditions

The *S. aureus* strains used in this study are listed in Table 1. *S. aureus* was cultured in 3 ml tryptic soy broth (TSB) in 30 ml universal tubes and grown for 15 to 17 h at 37 °C with shaking (180 rpm) to reach stationary phase. When necessary, TSB was supplemented with 10 µg ml^{-1} erythromycin or 90 µg ml^{-1} kanamycin. For daptomycin susceptibility assays, media was supplemented with a final concentration of 1.25 mM $CaCl_2$.

To generate TSB-grown bacteria, TSB was inoculated with 10^7 CFU ml^{-1} from overnight cultures and incubated at 37 °C with shaking (180 rpm) until 10^8 CFU ml^{-1} was reached (2-2.5 h depending on strain). To generate serum-adapted bacteria, these TSB-grown bacteria were centrifuged, resuspended in human serum from male AB plasma (Sigma) and incubated for 16 h at 37 °C with shaking (180 rpm). As *S. aureus* is unable to replicate in human serum, bacterial CFU counts of serum-adapted cultures were equal to those of TSB-grown cultures. Where necessary, serum was supplemented with sub-lethal concentrations of additional antibiotics; tunicamycin (128 µg ml^{-1}, Abcam), targocil (128 µg ml^{-1}, Cambridge Bioscience), tarocin A1 (64 µg ml^{-1}, Sigma), fosfomycin (64 µg ml^{-1}, Tokyo Chemical Industry) or verteporfin (10 – 80 µg ml^{-1}; Sigma). Where appropriate, serum was incubated for 2 h with polyclonal sheep IgG anti-LL-37 (2.5 – 20 µg ml_{-1}; R&D Systems) or anti-hNP-1 (2.5 – 20 µg ml_{-1}; R&D Systems) antibodies before serum-adaptation was carried out.

RPMI-adapted bacteria were generated by resuspending TSB-grown cultures in an equal volume of RPMI 1640 and incubating for 16 h at 37 °C with shaking (180 rpm). Where necessary, RPMI 1640 was supplemented with colistin (2.5 – 20 µg ml^{-1}, Sigma), LL-37 (5 – 40 µg ml^{-1}, R&D Systems), hNP-1 (0.625 – 10 µg ml^{-1}, Cambridge Bioscience) or dermcidin (12.5 – 100 µg ml^{-1}, Cambridge Bioscience).

Determination of antibiotic MICs

MICs were determined by broth microdilution as described previously[74]. Two-fold serial dilutions of antibiotics in TSB were generated in flat-bottomed 96-well plates. Wells were inoculated to a final concentration of 5 x 10^5 CFU ml^{-1} stationary phase *S. aureus* and incubated for 16 h at 37 □C under static conditions. The MIC was defined as the lowest concentration at which no visible growth was observed.

Antibiotic killing assays

3 ml cultures of 10^8 CFU ml^{-1} TSB-grown and serum/RMPI-adapted *S. aureus* were generated as described above. TSB-grown cultures were centrifuged and resuspended in human serum or RPMI 1640 immediately before the assay. When daptomycin killing assays were performed in RPMI 1640, $CaCl_2$ was added to a final concentration of 1.25 mM. The antibiotic or antimicrobial peptide of interest was added to these TSB-grown bacteria or to serum-adapted *S. aureus*. Cultures were incubated at 37˚C with shaking (180 rpm). At each time-point, aliquots were taken, serially diluted 10-fold in PBS in 96-well plates and plated to determine bacterial viability by CFU counts. Survival was calculated as a percentage of the starting inoculum.

Labelling of daptomycin with BoDipy fluorophore

Labelling of daptomycin with the BoDipy fluorophore was performed as described previously[75,76]. The primary amine group of daptomycin was used conjugate the antibiotic to the BoDipy fluorophore via its NHS ester. 100 µl 50 mg ml^{-1} daptomycin was incubated with 50 µl 10 mg ml^{-1} BoDipy FL SE (Thermo Fisher Scientific) and 850 µl 0.2 M sodium bicarbonate (pH 8.5) for 4 h at 37 □C. Unconjugated BoDipy was removed by dialysis against water at 4 □C using a Float-A-Lyzer G2 device with a 0.5 kDa molecular weight cut-off.

Measurements of daptomycin binding to *S. aureus*

To measure daptomycin binding to *S. aureus*, 3 ml TSB-grown or serum-adapted bacteria were generated as described above and incubated at 37 □C (shaking at 180 rpm) with 320 µg ml^{-1} BoDipy-labelled daptomycin in serum. Every 2 h, aliquots were taken, washed three times in PBS and then fluorescence was measured using a TECAN Infinite 200 PRO microplate reader (excitation 490 nm; emission 525 nm). Fluorescence values were blanked against uninoculated wells and divided by OD_{600} to normalise for cell density.

Fluorescence and phase-contrast microscopy

For measurements of daptomycin binding, TSB-grown or serum-adapted *S. aureus* were generated and incubated with BoDipy-daptomycin as described above. Samples were incubated with 10 µg ml^{-1} nile red for 10 mins at 37 □C to visualise cell membranes. Samples were washed 3 times in PBS and fixed in 4 % paraformaldehyde. For measurements of peptidoglycan synthesis, TSB-grown and serum-adapted *S. aureus* were generated as described above, but with the addition of 25 µM HADA at each step. Samples were washed 3 times in PBS and fixed in 4 % paraformaldehyde. For measurements of bacterial surface charge, 1 ml aliquots of TSB-grown and serum-adapted cultures of S. aureus were incubated with 80 µg ml^{-1} FITC-PLL for 10 min at room temperature in the dark. Cells were then washed three times in PBS and fixed in 4 % paraformaldehyde in the dark.

Aliquots (2 µl) of fixed bacteria were spotted onto microscope slides covered with a thin agarose layer (1.2 % agarose in water) and covered with a cover slip. Phase-contrast and fluorescence images were taken using a Zeiss Axio Imager.A1 microscope coupled to an AxioCam MRm and a 100× objective and processed using the Zen 2012 software (blue edition). BoDipy-daptomycin and FITC-PLL were detected using a green fluorescent protein filter set, Nile red fluorescence signals were detected using a Texas Red filter set and HADA using a DAPI filter set. Microscopy of all samples within an experiment were performed at the same time using identical settings to allow comparisons to be made between samples. The fluorescence intensities of individual cells were quantified using Zen 2012 software (blue edition).

Determination of membrane polarity

Membrane polarity was measured using 3,3'-dipropylthiadicarbocyanine iodide ($DiSC_3(5)$, Thermofisher Scientific) as described previously[77] with some modifications. 3 ml cultures of TSB-grown or serum-adapted *S. aureus* were generated as described above and incubated with 80 µg ml^{-1} daptomycin in human serum at 37˚C with shaking (180 rpm). After 6 h daptomycin exposure, 200 µl aliquots of cultures were added to black flat-bottomed 96-well plates. $DiSC_3(5)$ was added to a final concentration of 1 µM, mixed and the plate incubated statically at 37 °C for 5 minutes. Fluorescence was then measured using a TECAN Infinite 200 PRO microplate reader (excitation 622 nm; emission 670 nm). Fluorescence values were divided by OD_{600} measurements to normalise for cell density.

Determination of membrane permeability

Daptomycin-induced membrane permeability was measured using propidium iodide, a membrane-impermeant dye that fluoresces when bound to DNA, as described previously[78]. 3 ml cultures of TSB-grown or serum-adapted *S. aureus* were generated as described above and incubated with 80 µg ml^{-1}

[1] daptomycin in human serum at 37 ˚C with shaking (180 rpm). Aliquots were taken after 6 h daptomycin exposure and washed 3 times in PBS. 200 µl was transferred to a black-walled 96-well microtitre plate and PI was added to a final concentration of 2.5 µM. Fluorescence was measured using a TECAN Infinite 200 PRO microplate reader (excitation 535 nm; emission 617 nm). Fluorescence values were blanked against values from uninoculated wells and divided by OD_{600} to normalise for cell density.

Construction of strains

P*vraX-gfp* and P*dltA-gfp* plasmids were constructed using Gibson assembly to measure induction of VraSR and GraRS signalling respectively. To construct P*vraX-gfp,* t*he vraX* promoter was amplified from JE2 WT genomic DNA using primers *vraX*_Fw and *vraX*_Rev (Table 2). The pCN34 vector, together with *gfp*, was amplified from a previously constructed reporter plasmid[79] that contained a *recA* promoter-*gfp* construct using primers pCN34_*gfp*_Fw_*vraX* and pCN34_*gfp*_Rev_*vraX.* To construct P*dltA-gfp*, the *dltA* promoter was amplified from JE2 WT genomic DNA using primers *dltA*_Fw and *dltA*_Rev. The pCN34 vector, together with *gfp*, was amplified from a previously constructed reporter plasmid that contained a *recA* promoter-*gfp* construct[79] using primers pCN34_*gfp*_Fw_*dltA* and pCN34_*gfp*_Rev_*dltA.* Promoters were inserted into pCN34 upstream of *gfp* using Gibson assembly. Plasmids were transformed into *E. coli* DC10B, then electroporated into *S. aureus* RN4220 and finally transduced using ϕ11 into JE2 WT and the relevant mutant strain.

To construct the USA300 *ΔdltD* deletion mutant strain the *dltD* gene was replaced with an *erm* resistance marker in RN4220 *Δspa*[80]. A phage 85 lysate was made of the RN4220 *Δspa ΔdltD* strain and used to transduce USA300. Deletion of *dltD* was confirmed by PCR and sequencing.

Fluorescent reporter assays to determine induction of VraSR and GraRS signalling

Promoter-*gfp* constructs were used to measure gene expression in response to serum and LL-37 (5 – 80 µg ml^{-1}). To determine the response to serum, TSB-grown cultures were resuspended in serum and incubated at 37 ˚C. with shaking (180 rpm) in the dark for 6 h. At each time-point, 100 µl aliquots were removed, washed twice in PBS, resuspended in 100 µl PBS and transferred to a black 96-well plate. Fluorescence was measured at each time-point, and values were blanked against the fluorescence values of strains lacking the reporter construct.

To determine the response to LL-37, TSB-grown cultures (10 ml) were generated and resuspended in 100 µl PBS, resulting in a cell density of 10^{10} CFU ml^{-1}. A black-walled 96-well plate was prepared, with each well containing 200 µl RPMI 1640 supplemented with a range of concentrations of LL-37. Bacteria (2 µl) were inoculated into each well, resulting in an inoculum of 10^{8} CFU ml^{-1}.

The same approach was used to measure reporter activity in response to synthetic dermcidin (Cambridge Bioscience) or activated platelet supernatant from healthy donors. To generate this, whole human blood (30 ml) was collected in sodium citrate tubes (BD biosciences). Platelet rich plasma (PRP) was separated from red blood cells by centrifugation at 200 x g for 10 min. A second round of centrifugation 600 x g for 10 min collected the platelets, which were resuspended in RPMI 1640 (Thermo Fisher). $CaCl_2$ was added to a final concentration of 1.25 mM and platelets were incubated at 37 ˚C, with shaking (180 rpm) for 1 h until aggregation occurred. Tubes were centrifuged at 1,000 x g for 10 min to remove the activated platelets and the supernatant was centrifuged again at 1,000 x g for 10 min. The resulting supernatant was stored at -80˚C.

Plates containing peptide-exposed bacteria were inserted into a TECAN Infinite M200 PRO microplate reader and incubated at 37˚C for 16 h with orbital shaking (300 rpm). OD_{600} and fluorescence intensity (excitation 485 nm; emission 525 nm) were measured every 15 min. Fluorescence values were blanked against the fluorescence values of strains lacking the reporter construct. Blanked fluorescence values were divided by OD_{600} measurements to correct for changes in cell density which occurred during the assay.

WTA extraction and analysis

TSB-grown and serum-adapted bacteria were generated as described above and WTA was extracted as described previously[81]. 40 ml cultures were washed with 40 ml 50 mM MES (pH 6.5) (Buffer 1) and resuspended in 30 ml 50 mM MES (pH 6.5) supplemented with 4 % SDS (Buffer 2). Samples were boiled for 1 h and centrifuged before being washed twice in 2 ml Buffer 2, once in 2 ml 50 mM MES (pH 6.5) supplemented with 2 % NaCl (Buffer 3), and once in 2 ml Buffer 1. The pellet was resuspended in 1 ml 20 mM Tris-HCl pH 8, 0.5 % SDS and digested with 20 µg proteinase K for 4 h at 50 □C. The pellet was washed once with 1 ml Buffer 3, three times with 1 ml water, resuspended in 500 µl 0.1 M NaOH and incubated for 16 h at room temperature. After centrifugation, 500 µl supernatant was neutralised with 125 µl 1M Tris-HCl (pH 7.8) and analysed by PAGE. 10 µl aliquots of WTA samples were separated on a 20 % native polyacrylamide gel by electrophoresis using 0.1 M Tris, 0.1 M Tricine, pH 8.2 running buffer. Gels were then stained with alcian blue (1 mg/ml, 3 % acetic acid), destained with water and imaged using a Gel Doc EZ Imager (Bio-Rad). The phosphate content of WTA extracts was determined as described previously[82]. 6 N H_2SO_4, water, 2.5 % ammonium molybdate and 10 % ascorbic acid were mixed in a ratio of 1:2:1:1. 100 µl of this was mixed with 100 µl WTA extracts and then incubated at 37 □C for 90 mins. Phosphate concentrations were determined by measuring absorbance at 820 nm and correlating this to a standard curve generated from NaH_2PO_4 standards.

Quantification of D-alanine concentrations in WTA extracts

The amount of D-alanine modification present in WTA extracts was determined using a series of enzymatic reactions catalysed by D-amino acid oxidase and L-lactic dehydrogenase as described previously[83] with some modifications. Reactions were set up in a 96 well plate where each well contained 102 mM Tris-HCl (pH 8.5), 0.1875 U D-amino acid oxidase (Sigma), 20 U catalase (Sigma), 1.82 mg ml^{-1} β-NADH, 2 U L-lactic acid dehydrogenase and 20 µl WTA extract. Absorbance at 339 nm was measured before the addition of L-lactic acid dehydrogenase and then plates were incubated for 20 min at room temperature. A_{339} was measured again and the value at 20 min subtracted from the value at 0 min. A standard curve was generated using known D-alanine concentrations (0 – 100 µM) and used to interpolate the D-alanine concentrations in WTA extracts.

Extraction and purification of peptidoglycan

Peptidoglycan was extracted from 300 ml cultures of TSB-grown or serum-adapted cultures of *S. aureus*. Pellets were recovered by centrifugation at 3,200 x *g* for 10 min, pooled, transferred to a 50 ml falcon tube and snap frozen in liquid nitrogen. 4 % SDS (25 ml) was added to pellets and tubes were boiled in a beaker on a hot plate for 1 h. After cooling, pellets were recovered by centrifugation (3,200 x *g* for 10 min), moved to 2 ml Eppendorf tubes and washed 6 times with 2 ml distilled water (13,000 x *g* for 3 min). After the final wash, pellets were resuspended in 2 ml 10 mM Tris HCl (pH 7.4) containing 2 mg ml^{-1} pronase (Sigma). Tubes were incubated for 3 h at 60 ˚C to digest proteins. Samples were then resuspended in 30 ml 4 % SDS and boiled for 30 min to inactivate the pronase. Pellets were washed 6 times with distilled water and freeze-dried. The freeze-dried cell walls were resuspended in 1 M HCl at 10 mg ml^{-1}. Samples were incubated at 37 ˚C for 5 h to remove WTA from the peptidoglycan by hydrolysis. After recovering the peptidoglycan by centrifugation (13,000 x *g* for 3 min), pellets were washed 6 times in distilled water, freeze dried and weighed.

Rp-HPLC analysis of *S. aureus* peptidoglycan

Five milligrams of peptidoglycan were resuspended in 400 µl of 20 mM phosphate buffer (pH 6.0) and digested in the presence of 125 µg of mutanolysin for 16 h at 37 °C. Mutanolysin was inactivated for 5 min at 100 °C and soluble disaccharide-peptides were recovered following centrifugation at 20,000 x *g* for 10 min. After addition of one volume of 200 mM borate buffer (pH 9.25), muropeptides were reduced by the addition of 1 mg of sodium borohydride for 20 min at room temperature and the pH was adjusted to 4.5 with phosphoric acid.

For rp-HPLC analysis, the equivalent of 150 µg of soluble, reduced peptidoglycan fragments were injected on a Hypersil Gold aQ column (200 mm x 2.1 mm ID, 1.9 µm particles) equilibrated in 10

853 mM ammonium phosphate (pH 5.5) (buffer A) at a flow rate of 0.3 ml min^{-1}. Muropeptides were
854 eluted with a 25 min gradient to 25 % methanol in buffer A. Detection was carried out by monitoring
855 absorbance at 210 nm.

856

857

858 **Triton X-100 induced lysis**

859 Cultures of TSB-grown and serum-adapted *S. aureus* were generated as described above, washed
860 twice in PBS and resuspended in PBS supplemented with 0.05 % Triton X-100. 200 µl aliquots (at 10^8
861 CFU ml^{-1}) were transferred to flat-bottomed 96-well plates, incubated at 30 °C and OD_{600} measured
862 every 15 mins for 6 h. Values were blanked against uninoculated wells and calculated as a
863 percentage of the starting value.

864 **Analysis of cell wall hydrolase activity by zymography**

865 10 ml cultures of TSB-grown or serum-adapted *S. aureus* were generated as described above,
866 resuspended in 1 ml 50 mM Tris-HCl (pH 7.5) containing 20 % sucrose, 10 mM $MgCl_2$ and 0.1 µg ml^{-1}
867 lysostaphin and incubated at 37 ˚C for 1 h. Samples were centrifuged (8000 x *g,* 3 mins) and
868 supernatants (containing cell wall fragments) were analysed by SDS-PAGE using 10 % polyacrylamide
869 gels containing autoclaved *S. aureus* which were prepared as described previously. Gels were
870 washed in water, incubated overnight at 37˚C in renaturation buffer (50 mM Tris-HCl (pH 7.5), 0.1 %
871 Triton X-100, 10 mM $CaCl_2$, 10 mM $MgCl_2$), stained with 0.1 % methylene blue in 0.01 % KOH for 1 h
872 at room temperature and destained overnight with water.

873 **Lipid extraction and thin layer chromatography**

874 Lipids were extracted from TSB-grown (10 ml) and serum-adapted (10 ml) cultures using a method
875 based on that of Bligh and Dyer[53,54]. Cells were washed twice with PBS, twice with 0.1 % Triton X-100
876 and twice with PBS to remove unincorporated serum-derived lipids[33] before resuspension in 300 µl 2
877 % NaCl. After addition of 0.2 mg ml^{-1} lysostaphin, cells were incubated at 37 □C for 10 min. 1 ml
878 chloroform-methanol (2:1; v/v) was added, vortexed for 2 min and incubated at room temperature
879 for 30 min. Chloroform (300 µl) and 2 % NaCl (300 µl) were added, and after centrifugation, the
880 lower layer was recovered and evaporated at room temperature. Samples were resuspended in 100
881 µl chloroform-methanol (2:1; v/v) and separated by one-dimensional TLC. Equal volumes of lipid
882 extracts were spotted onto silica 60 F254 HPTLC plates (Merck) and migrated with
883 chloroform:methanol:ammonium hydroxide (30 %) (65:30:4; v/v/v). After drying, TLC plates were

sprayed with $CuSO_4$ (100 mg ml^{-1}) in 8 % phosphoric acid and heated at 180 □C. Signal intensities were quantified using ImageJ.

Construction of *S. aureus* complementation strains

S. aureus mutants were complemented using the multi-copy *E. coli*/*S. aureus* shuttle vector pCN34[84] containing the relevant gene/operon along with its promoter and terminator regions. All genes were amplified from USA300 LAC* genomic DNA and were inserted into pCN34 at the multiple cloning site using Gibson assembly. Primer sequences used to generate complementation strains are shown in Table 2.

The *vraUTSR* operon, together with 500 bp regions up and downstream of the operon, was amplified using primers *vraUTSR*_Fw and *vraUTSR*_Rev. The pCN34 vector was amplified using primers pCN34_Fw_*vra* and pCN34_Rev_*vra*. The *graXRS* operon, together with 500 bp regions up and downstream of the operon, was amplified using primers *graXRS*_Fw and *graXRS*_Rev. The pCN34 vector was amplified using primers pCN34_Fw_*gra* and pCN34_Rev_*gra*. The *dltD* gene and the *dlt* operon promoter (present in the 500 bp region upstream of *dltA*) were amplified separately. *dltD,* together with a 500 bp region downstream of *dltD,* was amplified using primers *dltD*_Fw and *dltD*_Rev. The 500 bp region upstream of *dltA* was amplified using primers *dlt*_pro_Fw and *dlt*_pro_Rev. The pCN34 vector was amplified using primers pCN34_Fw_*dlt* and pCN34_Rev_*dlt.* The *cls2* gene, along with upstream and downstream regions, was amplified using primers *cls2*_Fw and *cls2*_Rev. The pCN34 vector was amplified using primers pCN34_Fw_*cls2* and pCN34_Rev_*cls2*.

After amplification, fragments were assembled using Gibson assembly, transformed into the *E. coli* strain DH5α, electroporated into the restriction-deficient *S. aureus* strain RN4220 and transduced (along with empty pCN34 as a control) by phage ϕ11 into the relevant mutant.

Statistical analyses

Data are represented as the mean ± standard deviations from three or more independent experiments and were analysed by Student's t test, one-way ANOVA or two-way ANOVA with appropriate *post-hoc* multiple comparison test using GraphPad Prism (V8.0), as described in the figure legends.

Acknowledgements

Angelika Grundling and Nathalie Reichmann (Imperial College London) are thanked for providing strains. Vladimir Pelicic (Imperial College London) is thanked for providing access to the fluorescent

microscope. Simon Foster (University of Sheffield) is thanked for providing HADA. EVKL was supported by a Wellcome Trust PhD Studentship (203812/Z/16/Z). AME acknowledges funding from the Rosetrees Trust and from the Imperial NIHR Biomedical Research Centre, Imperial College London. All authors acknowledge the provision of strains by the Network on Antimicrobial Resistance in Staphylococcus aureus (NARSA) Program: under NIAID/ NIH Contract No. HHSN272200700055C. The funders had no role in the study design, interpretation of the findings or the writing of the manuscript.

Conflict of interest statement

The authors declare no conflict of interest.

Table 1. Bacterial strains

Strain	Description	Reference or source
Staphylococcus aureus		
USA300 LAC*	LAC strain of the USA300 CA-MRSA lineage, cured of LAC-p03 plasmid	[85]
USA300 LAC* *ΔdltD*	USA300 LAC* with the *dltD* gene deleted, Ery^r	This study
USA300 LAC* *ΔdltD* pCN34	USA300 LAC* Δ*dltD* carrying the empty pCN34 vector, Ery^r Kan^r	This study
USA300 LAC* *ΔdltD* P*dltD*	USA300 LAC* Δ*dltD* complemented with P*dltD,* Ery^r Kan^r	This study
USA300 LAC JE2	LAC strain of the USA300 CA-MRSA lineage cured of plasmids	[41]
USA300 LAC JE2 *agrC*::Tn	USA300 LAC JE2 with a *bursa aurealis* transposon insertion in *agrC*, Ery^r	[41]
USA300 LAC JE2 *saeS*::Tn	USA300 LAC JE2 with a *bursa aurealis* transposon insertion in *saeS*, Ery^r	[41]
USA300 LAC JE2 *arlS*::Tn	USA300 LAC JE2 with a *bursa aurealis* transposon insertion in *arlS*, Ery^r	[41]
USA300 LAC JE2 *lytS*::Tn	USA300 LAC JE2 with a *bursa aurealis* transposon insertion in *lytS*, Ery^r	[41]
USA300 LAC JE2 *srrB*::Tn	USA300 LAC JE2 with a *bursa aurealis* transposon insertion in *srrB*, Ery^r	[41]
USA300 LAC JE2 *nreB*::Tn	USA300 LAC JE2 with a *bursa aurealis* transposon insertion in *nreB*, Ery^r	[41]
USA300 LAC JE2 *airS*::Tn	USA300 LAC JE2 with a *bursa aurealis* transposon insertion in *airS*, Ery^r	[41]
USA300 LAC JE2 *hptS*::Tn	USA300 LAC JE2 with a *bursa aurealis* transposon insertion in *hptS*, Ery^r	[41]
USA300 LAC JE2 *hssS*::Tn	USA300 LAC JE2 with a *bursa aurealis* transposon insertion in *hssS*, Ery^r	[41]
USA300 LAC JE2 *kdpD*::Tn	USA300 LAC JE2 with a *bursa aurealis* transposon insertion in *kdpD*, Ery^r	[41]

USA300 LAC JE2 *phoP*::Tn	USA300 LAC JE2 with a *bursa aurealis* transposon insertion in *phoP*, Ery^r	[41]
USA300 LAC JE2 *vraS*::Tn	USA300 LAC JE2 with a *bursa aurealis* transposon insertion in *vraS*, Ery^r	[41]
USA300 LAC JE2 *graS*::Tn	USA300 LAC JE2 with a *bursa aurealis* transposon insertion in *graS*, Ery^r	[41]
USA300 LAC JE2 *braS*::Tn	USA300 LAC JE2 with a *bursa aurealis* transposon insertion in *braS*, Ery^r	[41]
USA300 LAC JE2 *desK*::Tn	USA300 LAC JE2 with a *bursa aurealis* transposon insertion in *desK*, Ery^r	[41]
USA300 LAC JE2 *graS*::Tn pCN34	USA300 LAC JE2 *graS*::Tn carrying the empty pCN34 plasmid, Ery^r Kan^r	This study
USA300 LAC JE2 *graS*::Tn P*graXRS*	USA300 LAC JE2 *graS*::Tn complemented with P*graXRS*, Ery^r Kan^r	This study
USA300 LAC JE2 P*dltA-gfp*	USA300 LAC JE2 carrying the P*dltA-gfp* reporter plasmid, Kan^r	This study
USA300 LAC JE2 *graS*::Tn P*dltA-gfp*	USA300 LAC JE2 *graS*::Tn carrying the P*dltA-gfp* reporter plasmid, Ery^r Kan^r	This study
USA300 LAC JE2 *vraS*:Tn pCN34	USA300 LAC JE2 *vraS*::Tn carrying the empty pCN34 plasmid, Ery^r Kan^r	This study
USA300 LAC JE2 *vraS*:Tn P*vraUTSR*	USA300 LAC JE2 *vraS*::Tn complemented with P*vraUTSR*, Ery^r Kan^r	This study
USA300 LAC JE2 P*vraX-gfp*	USA300 LAC JE2 carrying the P*vraX-gfp* reporter plasmid, Kan^r	This study
USA300 LAC JE2 *vraS*::Tn P*vraX-gfp*	USA300 LAC JE2 *vraS*::Tn carrying the P*vraX-gfp* reporter plasmid, Ery^r Kan^r	This study
USA300 LAC JE2 *mprF*::Tn	USA300 LAC JE2 with a *bursa aurealis* transposon insertion in *mprF*, Ery^r	[41]
USA300 LAC JE2 *cls1*::Tn	USA300 LAC JE2 with a *bursa aurealis* transposon insertion in *cls1*, Ery^r	[41]
USA300 LAC JE2 *cls2*::Tn	USA300 LAC JE2 with a *bursa aurealis* transposon insertion in *cls2*, Ery^r	[41]
USA300 LAC JE2 *cls2*::Tn pCN34	USA300 LAC JE2 *cls2*::Tn carrying the empty pCN34 vector, Ery^r Kan^r	This study
USA300 LAC JE2 *cls2*::Tn P*cls2*	USA300 LAC JE2 *cls2*::Tn complemented with P*cls2*, Ery^r Kan^r	This study

Table 2. Primers

Oligonucleotide	Sequence (5'-3')
For construction of P*vraX-gfp* fluorescent reporter plasmid:	
pCN34_*gfp*_Fw _*vraX*	AGCAAAGGAGGTAATATAGGAAAAAAAATGAGTAAAGGAGAAGAACTTTTC ACTGG
pCN34_*gfp*_Rev_*vraX*	GTTGTATGCACCGTGATCCAGTGTCATCTGAACCATAGGATCCTCT
*vraX*_Fw	TCCTATGGTTCAGATGACACTGGATCACGGTGCATACAACCG
*vraX*_rev	CTCCTTTACTCATTTTTTTTCCTATATTACCTCCTTTGCTACTCTATGG
For construction of P*dltA-gfp* fluorescent reporter plasmid:	
pCN34_*gfp*_Fw_*dltA*	TCTAATGAGGGAGACTTAATAAAAAAAATGAGTAAAGGAGAAGAAC
pCN34_*gfp*_Rev_*dltA*	AATTATCATCAGCGCAAATAGTGTCATCTGAACCATAGGA
*dltA*_Fw	TCCTATGGTTCAGATGACACTATTTGCGCTGATGATAATTCA
*dltA*_Rev	TCTCCTTTACTCATTTTTTTTATTAAGTCTCCCTCATTAGAACT
For construction of P*vraUTSR* complementation plasmid*:*	
pCN34_Fw_*vra*	TATGTTTTAGAATAGTTACCACAACGTCGTGACTGGGAAA
pCN34_Rev_*vra*	TAAGTTTTTAATGACTTTCAAAAACGACGGCCAGTGAATT
*vraUTSR*_Fw	AATTCACTGGCCGTCGTTTTTGAAAGTCATTAAAAACTTAACAGG
*vraUTSR*_Rev	TTTCCCAGTCACGACGTTGTGGTAACTATTCTAAAACATATGGCA
For construction of P*graXRS* complementation plasmid*:*	
pCN34_Fw_*gra*	AGAAGTTAGATAAAGAACATACAACGTCGTGACTGGGAAA
pCN34_Rev_*gra*	AAATGTACCACTCAATAACCAAAACGACGGCCAGTGAATT
*graXRS*_Fw	AATTCACTGGCCGTCGTTTTGGTTATTGAGTGGTACATTTGC
*graXRS*_Rev	TTTCCCAGTCACGACGTTGTATGTTCTTTATCTAACTTCTGTACC
For construction of P*dltD* complementation plasmid*:*	
pCN34_Fw_*dlt*	TATCTTTATAGGCGCCTTTGCGGAAAGAG
pCN34_Rev_*dlt*	AGCGCAAATAATTCGCCATTCAGGCTGC
*dltA*_pro_Fw	AATGGCGAATTATTTGCGCTGATGATAATTC
*dltA*_pro_Rev	TTAATTTCATATTAAGTCTCCCTCATTAGAAC
*dltD*_Fw	GAGACTTAATATGAAATTAAAACCTTTTTTACCC
*dltD*_Rev	CAAAGGCGCCTATAAAGATATTAAGTTAACAGAACATATTATG
For construction of P*cls2* complementation plasmid*:*	
pCN34_Fw_*cls2*	GGCGCCTTTGCGGAAAGAG
pCN34_Rev_*cls2*	ATTCGCCATTCAGGCTGC
*cls2*_Fw	AGCCTGAATGGCGAATCTGTTTAACGCCGAACGTG
*cls2*_Rev	TTCCGCAAAGGCGCCTTTCGTCAACGGTATCATGAAG

References

1. Public Health England. Annual epidemiological commentary: bacteraemia, MSSA bacteraemia and C . difficile infections, up to and including financial year April 2018 to March 2019. 1–88 (2019).

2. Nathwani, D. *et al.* Guidelines for UK practice for the diagnosis and management of methicillin-resistant Staphylococcus aureus (MRSA) infections presenting in the community. *J. Antimicrob. Chemother.* **61**, 976–994 (2008).

3. Taylor, S. D. & Palmer, M. The action mechanism of daptomycin. *Bioorganic Med. Chem.* **24**, 6253–6268 (2016).

4. Pujol, M. *et al.* Daptomycin Plus Fosfomycin Versus Daptomycin Alone for Methicillin-resistant Staphylococcus aureus Bacteremia and Endocarditis: A Randomized Clinical Trial. *Clin. Infect. Dis.* 1–9 (2020) doi:10.1093/cid/ciaa1081.

5. Tong, S. Y. C. *et al.* Effect of Vancomycin or Daptomycin with vs Without an Antistaphylococcal β-Lactam on Mortality, Bacteremia, Relapse, or Treatment Failure in Patients with MRSA Bacteremia: A Randomized Clinical Trial. *JAMA - J. Am. Med. Assoc.* **323**, 527–537 (2020).

6. Chong, Y. P. *et al.* Persistent staphylococcus aureus bacteremia: A prospective analysis of risk factors, outcomes, and microbiologic and genotypic characteristics of isolates. *Med. (United States)* **92**, 98–108 (2013).

7. Vos, F. J. *et al.* Metastatic infectious disease and clinical outcome in Staphylococcus aureus and Streptococcus species bacteremia. *Medicine (Baltimore).* **91**, 86–94 (2012).

8. Thampi, N. *et al.* Multicenter study of health care cost of patients admitted to hospital with Staphylococcus aureus bacteremia: Impact of length of stay and intensity of care. *Am. J. Infect. Control* **43**, 739–744 (2015).

9. Blot, S. I., Vandewoude, K. H., Hoste, E. A. & Colardyn, F. A. Outcome and attributable mortality in critically ill patients with bacteremia involving methicillin-susceptible and methicillin-resistant Staphylococcus aureus. *Arch. Intern. Med.* **162**, 2229–2235 (2002).

10. Andrew Seaton, R. *et al.* Real-world daptomycin use across wide geographical regions: Results from a pooled analysis of CORE and EU-CORE. *Ann. Clin. Microbiol. Antimicrob.* **15**, 1–11 (2016).

11. Moise, P. A. *et al.* Multicenter evaluation of the clinical outcomes of daptomycin with and without concomitant β-lactams in patients with staphylococcus aureus bacteremia and mild to moderate renal impairment. *Antimicrob. Agents Chemother.* **57**, 1192–1200 (2013).

12. Kuehl, R., Morata, L., Meylan, S., Mensa, J. & Soriano, A. When antibiotics fail: A clinical and microbiological perspective on antibiotic tolerance and persistence of Staphylococcus aureus. *J. Antimicrob. Chemother.* **75**, 1071–1086 (2020).

13. Dombrowski, J. C. & Winston, L. G. Clinical failures of appropriately-treated methicillin-resistant Staphylococcus aureus infections. *J. Infect.* (2008) doi:10.1016/j.jinf.2008.04.003.

14. Brauner, A., Fridman, O., Gefen, O. & Balaban, N. Q. Distinguishing between resistance, tolerance and persistence to antibiotic treatment. *Nature Reviews Microbiology* (2016) doi:10.1038/nrmicro.2016.34.

15. Mechler, L. *et al.* A novel point mutation promotes growth phase-dependent daptomycin tolerance in Staphylococcus aureus. *Antimicrob. Agents Chemother.* **59**, 5366–5376 (2015).

16. Barros, E. *et al.* Daptomycin Resistance and Tolerance Due to Loss of Function in Staphylococcus aureus dsp1 and asp23. *Antimicrob. Agents Chemother.* **63**, 1–12 (2018).

17. Berti, A. D. *et al.* Daptomycin selects for genetic and phenotypic adaptations leading to antibiotic tolerance in MRSA. *J. Antimicrob. Chemother.* **73**, 2030–2033 (2018).

18. Westblade, L. F., Errington, J. & Dörr, T. Antibiotic tolerance. *PLoS Pathog.* (2020) doi:10.1371/journal.ppat.1008892.

19. Windels, E. M., Michiels, J. E., van den Bergh, B., Fauvart, M. & Michiels, J. Antibiotics: Combatting tolerance to stop resistance. *MBio* (2019) doi:10.1128/mBio.02095-19.

20. Lopatkin, A. J. *et al.* Bacterial metabolic state more accurately predicts antibiotic lethality than growth rate. *Nature Microbiology* (2019) doi:10.1038/s41564-019-0536-0.

21. Mascio, C. T. M., Alder, J. D. & Silverman, J. A. Bactericidal action of daptomycin against

stationary-phase and nondividing Staphylococcus aureus cells. *Antimicrob. Agents Chemother.* **51**, 4255–4260 (2007).

22. Tkachenko, A. G. Stress Responses of Bacterial Cells as Mechanism of Development of Antibiotic Tolerance (Review). *Appl. Biochem. Microbiol.* (2018) doi:10.1134/S0003683818020114.

23. Haaber, J. *et al.* Reversible antibiotic tolerance induced in Staphylococcus aureus by concurrent drug exposure. *MBio* (2015) doi:10.1128/mBio.02268-14.

24. Hobbs, J. K. & Boraston, A. B. (p)ppGpp and the Stringent Response: An Emerging Threat to Antibiotic Therapy. *ACS Infect. Dis.* (2019) doi:10.1021/acsinfecdis.9b00204.

25. Peyrusson, F. *et al.* Intracellular Staphylococcus aureus persisters upon antibiotic exposure. *Nat. Commun.* **11**, (2020).

26. Bui, L. M. G., Conlon, B. P. & Kidd, S. P. Antibiotic tolerance and the alternative lifestyles of Staphylococcus aureus. *Essays Biochem.* **61**, 71–79 (2017).

27. Corrigan, R. M., Bellows, L. E., Wood, A. & Gründling, A. PpGpp negatively impacts ribosome assembly affecting growth and antimicrobial tolerance in Grampositive bacteria. *Proc. Natl. Acad. Sci. U. S. A.* **113**, E1710–E1719 (2016).

28. Ranganathan, N., Johnson, R. & Edwards, A. M. The general stress response of staphylococcus aureus promotes tolerance of antibiotics and survival in whole human blood. *Microbiol. (United Kingdom)* **166**, 1088–1094 (2020).

29. Friberg, C. *et al.* Human antimicrobial peptide, LL-37, induces non-inheritable reduced susceptibility to vancomycin in Staphylococcus aureus. *Sci. Rep.* **10**, 1–8 (2020).

30. Rowe, S. *et al.* Reactive oxygen species induce antibiotic tolerance during systemic Staphylococcus aureus infection. *Nat. Microbiol.* **5**, 282–290 (2020).

31. Beam, J. E. *et al.* Macrophage-Produced Peroxynitrite Induces Antibiotic Tolerance and Supersedes Intrinsic Mechanisms of Persister Formation. *Infect. Immun.* (2021) doi:10.1128/iai.00286-21.

32. Rowe, S. E., Beam, J. E. & Conlon, B. P. Recalcitrant Staphylococcus aureus infections: Obstacles and solutions. *Infect. Immun.* (2021) doi:10.1128/IAI.00694-20.

33. Hines, K. M. *et al.* Lipidomic and Ultrastructural Characterization of the Cell Envelope of Staphylococcus aureus Grown in the Presence of Human Serum . *mSphere* **5**, 1–16 (2020).

34. Sen, S. *et al.* Growth-environment dependent modulation of Staphylococcus aureus branched-chain to straight-chain fatty acid ratio and incorporation of unsaturated fatty acids. *PLoS One* **11**, 1–17 (2016).

35. Sutton, J. A. F. *et al.* Staphylococcus aureus cell wall structure and dynamics during host-pathogen interaction. *PLOS Pathog.* **17**, e1009468 (2021).

36. Boudjemaa, R. *et al.* Failure of daptomycin to kill Staphylococcus aureus: impact of bacterial membrane fatty acid composition. *Antimicrob. Agents Chemother.* AAC.00023-18 (2018) doi:10.1128/AAC.00023-18.

37. Diekema, D. J. *et al.* The microbiology of bloodstream infection: 20-year trends from the SENTRY antimicrobial surveillance program. *Antimicrob. Agents Chemother.* **63**, 1–10 (2019).

38. Ehrenkranz, N. J., Elliott, D. F. & Zarco, R. Serum Bacteriostasis of Staphylococcus aureus. *Infect. Immun.* **3**, 664–670 (1971).

39. Dvorchik, B. H., Brazier, D., DeBruin, M. F. & Arbeit, R. D. Daptomycin pharmacokinetics and safety following administration of escalating doses once daily to healthy subjects. *Antimicrob. Agents Chemother.* **47**, 1318–1323 (2003).

40. te Winkel, J. D., Gray, D. A., Seistrup, K. H., Hamoen, L. W. & Strahl, H. Analysis of antimicrobial-triggered membrane depolarization using voltage sensitive dyes. *Front. Cell Dev. Biol.* **4**, 1–10 (2016).

41. Fey, P. D. *et al.* A Genetic Resource for Rapid and Comprehensive Phenotype. *MBio* **4**, e00537-12 (2013).

42. Utaida, S. *et al.* Genome-wide transcriptional profiling of the response of Staphylococcus aureus to cell-wall-active antibiotics reveals a cell-wall-stress stimulon. *Microbiology* **149**, 2719–2732 (2003).

43. Dengler, V., Meier, P. S., Heusser, R., Berger-Bächi, B. & McCallum, N. Induction kinetics of the Staphylococcus aureus cell wall stress stimulon in response to different cell wall active antibiotics. *BMC Microbiol.* **11**, 16 (2011).

44. Cheung, A. L. *et al.* Site-specific mutation of the sensor kinase gras in Staphylococcus aureus alters the adaptive response to distinct cationic antimicrobial peptides. *Infect. Immun.* **82**, 5336–5345 (2014).

45. Prieto, J. M. *et al.* Inhibiting the two-component system GraXRS with verteporfin to combat

1048 Staphylococcus aureus infections. *Sci. Rep.* **10**, 1–12 (2020).

1049 46. Li, M. *et al.* The antimicrobial peptide-sensing system aps of Staphylococcus aureus. *Mol.*
1050 *Microbiol.* **66**, 1136–1147 (2007).

1051 47. Herbert, S. *et al.* Molecular basis of resistance to muramidase and cationic antimicrobial
1052 peptide activity of lysozyme in staphylococci. *PLoS Pathog.* **3**, 0981–0994 (2007).

1053 48. Meehl, M., Herbert, S., Götz, F. & Cheung, A. Interaction of the GraRS two-component system
1054 with the VraFG ABC transporter to support vancomycin-intermediate resistance in
1055 Staphylococcus aureus. *Antimicrob. Agents Chemother.* **51**, 2679–2689 (2007).

1056 49. Tran, T. T. *et al.* Mechanisms of Drug Resistance: Daptomycin Resistance. *Ann. N. Y. Acad. Sci .*
1057 **1354**, 32–53 (2015).

1058 50. Falord, M., Mäder, U., Hiron, A., Dbarbouillé, M. & Msadek, T. Investigation of the
1059 Staphylococcus aureus GraSR regulon reveals novel links to virulence, stress response and cell
1060 wall signal transduction pathways. *PLoS One* **6**, (2011).

1061 51. Kuru, E., Tekkam, S., Hall, E., Brun, Y. V. & Van Nieuwenhze, M. S. Synthesis of fluorescent D-
1062 amino acids and their use for probing peptidoglycan synthesis and bacterial growth in situ.
1063 *Nat. Protoc.* **10**, 33–52 (2015).

1064 52. Mollner, S. & Braun, V. Murein hydrolase (N-acetyl-muramyl-l-alanine amidase) in human
1065 serum. *Arch. Microbiol.* (1984) doi:10.1007/BF00454921.

1066 53. Bligh, E. G. & Dyer, W. J. A rapid method of total lipid extraction and purification. *Can. J.*
1067 *Biochem. Physiol.* **37**, 911–917 (1959).

1068 54. Tsai, M. *et al.* Staphylococcus aureus requires cardiolipin for survival under conditions of high
1069 salinity. *BMC Microbiol.* **11**, 13 (2011).

1070 55. Kuhn, S., Slavetinsky, C. J. & Peschel, A. Synthesis and function of phospholipids in
1071 Staphylococcus aureus. *Int. J. Med. Microbiol.* **305**, 196–202 (2015).

1072 56. Dürr, U. H. N., Sudheendra, U. S. & Ramamoorthy, A. LL-37, the only human member of the
1073 cathelicidin family of antimicrobial peptides. *Biochim. Biophys. Acta - Biomembr.* **1758**, 1408–
1074 1425 (2006).

1075 57. Kraus, D. *et al.* The GraRS regulatory system controls Staphylococcus aureus susceptibility to
1076 antimicrobial host defenses. *BMC Microbiol.* **8**, 1–5 (2008).

58. Cui, L., Tominaga, E., Neoh, H. M. & Hiramatsu, K. Correlation between reduced daptomycin susceptibility and vancomycin resistance in vancomycin-intermediate Staphylococcus aureus. *Antimicrob. Agents Chemother.* **50**, 1079–1082 (2006).

59. Yang, S. J. *et al.* Cell wall thickening is not a universal accompaniment of the daptomycin nonsusceptibility phenotype in Staphylococcus aureus: Evidence for multiple resistance mechanisms. *Antimicrob. Agents Chemother.* **54**, 3079–3085 (2010).

60. Gaupp, R. *et al.* Staphylococcus aureus metabolic adaptations during the transition from a daptomycin susceptibility phenotype to a daptomycin nonsusceptibility phenotype. *Antimicrob. Agents Chemother.* **59**, 4226–4238 (2015).

61. Bertsche, U. *et al.* Correlation of daptomycin resistance in a clinical Staphylococcus aureus strain with increased cell wall teichoic acid production and D-alanylation. *Antimicrob. Agents Chemother.* **55**, 3922–3928 (2011).

62. Bertsche, U. *et al.* Increased Cell Wall Teichoic Acid Production and D-alanylation Are Common Phenotypes among Daptomycin-Resistant Methicillin-Resistant Staphylococcus aureus (MRSA) Clinical Isolates. *PLoS One* **8**, 1–11 (2013).

63. Jiang, J., Bhuiyan, S., Shen, H., Cameron, D. R. & Rupasinghe, T. W. T. Antibiotic resistance and host immune evasion in Staphylococcus aureus mediated by a metabolic adaptation. **116**, (2019).

64. Zhang, T. H. *et al.* Cardiolipin prevents membrane translocation and permeabilization by daptomycin. *J. Biol. Chem.* (2014) doi:10.1074/jbc.M114.554444.

65. Hernández-Villa, L. *et al.* Biophysical evaluation of cardiolipin content as a regulator of the membrane lytic effect of antimicrobial peptides. *Biophys. Chem.* (2018) doi:10.1016/j.bpc.2018.04.001.

66. Koprivnjak, T. *et al.* Characterization of Staphylococcus aureus cardiolipin synthases 1 and 2 and their Contribution to accumulation of cardiolipin in stationary phase and within phagocytes. *J. Bacteriol.* **193**, 4134–4142 (2011).

67. El-Halfawy, O. M. *et al.* Discovery of an antivirulence compound that reverses β-lactam resistance in MRSA. *Nat. Chem. Biol.* **16**, 143–149 (2020).

68. García-de-la-Mària, C. *et al.* The Combination of Daptomycin and Fosfomycin Has Synergistic, Potent, and Rapid Bactericidal Activity against Methicillin-Resistant Staphylococcus aureus in a Rabbit Model of Experimental Endocarditis . *Antimicrob. Agents Chemother.* (2018)

doi:10.1128/aac.02633-17.

69. Lingscheid, T. *et al.* Daptomycin plus fosfomycin, a synergistic combination in experimental implant-associated osteomyelitis due to methicillin-resistant Staphylococcus aureus in rats. *Antimicrob. Agents Chemother.* **59**, 859–863 (2015).

70. Aktas, G. & Derbentli, S. In vitro activity of daptomycin combinations with rifampicin, gentamicin, fosfomycin and fusidic acid against MRSA strains. *J. Glob. Antimicrob. Resist.* (2017) doi:10.1016/j.jgar.2017.05.022.

71. Garrigós, C. *et al.* Fosfomycin-daptomycin and other fosfomycin combinations as alternative therapies in experimental foreign-body infection by methicillin-resistant Staphylococcus aureus. *Antimicrob. Agents Chemother.* **57**, 606–610 (2013).

72. Mishra, N. N. *et al.* Synergy mechanisms of daptomycin-fosfomycin combinations in daptomycin-susceptible and -resistant methicillin-resistant S. aureus: in vitro, ex vivo and in vivo metrics. *Antimicrob. Agents Chemother.* (2021) doi:10.1128/AAC.01649-21.

73. Snyder, A. D. H. *et al.* Fosfomycin enhances the activity of Daptomycin against Vancomycin-Resistant enterococci in an in Vitro pharmacokinetic-pharmacodynamic model. *Antimicrob. Agents Chemother.* **60**, 5716–5723 (2016).

74. Wiegand, I., Hilpert, K. & Hancock, R. E. W. Agar and broth dilution methods to determine the minimal inhibitory concentration (MIC) of antimicrobial substances. *Nat. Protoc.* (2008) doi:10.1038/nprot.2007.521.

75. Pader, V. *et al.* Staphylococcus aureus inactivates daptomycin by releasing membrane phospholipids. *Nat. Microbiol.* (2016) doi:10.1038/nmicrobiol.2016.194.

76. Ledger, E. V. K., Pader, V. & Edwards, A. M. Enterococcus faecalis and pathogenic streptococci inactivate daptomycin by releasing phospholipids. *Microbiol. (United Kingdom)* (2017) doi:10.1099/mic.0.000529.

77. te Winkel, J. D., Gray, D. A., Seistrup, K. H., Hamoen, L. W. & Strahl, H. Analysis of antimicrobial-triggered membrane depolarization using voltage sensitive dyes. *Front. Cell Dev. Biol.* **4**, 1–10 (2016).

78. Clementi, E. A., Marks, L. R., Roche-Håkansson, H. & Håkansson, A. P. Monitoring changes in membrane polarity, membrane integrity, and intracellular ion concentrations in Streptococcus pneumoniae using fluorescent dyes. *J. Vis. Exp.* (2014) doi:10.3791/51008.

79. Ha, K. P. *et al.* Staphylococcal dna repair is required for infection. *MBio* **11**, 1–18 (2020).

80. Reichmann, N. T. Interaction and localisation studies of the lipoteichoic acid synthesis proteins in Staphylococcus aureus. (Imperial College London, 2012). doi:https://doi.org/10.25560/39406.

81. Kho, K. & Meredith, T. Extraction and Analysis of Bacterial Teichoic Acids. *BIO-PROTOCOL* (2018) doi:10.21769/bioprotoc.3078.

82. Chan, Y. G. Y., Frankel, M. B., Dengler, V., Schneewind, O. & Missiakasa, D. Staphylococcus aureus mutants lacking the lytr-cpsa-Psr family of enzymes release cell wall teichoic acids into the extracellular medium. *J. Bacteriol.* **195**, 4650–4659 (2013).

83. Watababe, A. *et al.* Role of lysine 39 of alanine racemase from Bacillus stearothermophilus that binds pyridoxal 5'-phosphate: Chemical rescue studies of Lys39 → Ala mutant. *J. Biol. Chem.* **274**, 4189–4194 (1999).

84. Charpentier, E. *et al.* Novel cassette-based shuttle vector system for gram-positive bacteria. *Appl. Environ. Microbiol.* **70**, 6076–6085 (2004).

85. Boles, B. R., Thoende, M., Roth, A. J. & Horswill, A. R. Identification of genes involved in polysaccharide- independent Staphylococcus aureus biofilm formation. *PLoS One* **5**, (2010).

1201

1202

1203

1204

1205

1206

1207

1208

1209

1210

1211

1212

1213